

Geological Structure and Late Quaternary Geomorphological Evolution of the Farasan Islands Continental Shelf, South Red Sea, SW Saudi Arabia

Dimitris Sakellariou, Grigoris Rousakis, Ioannis Panagiotopoulos, Ioannis Morfis, and Geoff N. Bailey

Abstract

A marine geological-geophysical survey of selected areas on the Saudi Arabian continental shelf of the Farasan Archipelago in the southeastern Red Sea has been conducted in the framework of the ERC-funded DISPERSE project. The aim was to explore systematically the geological, tectonic and sedimentary structure of the shelf and provide insights into the submerged prehistoric landscapes. The survey targeted features believed to be of significance in relation to the archaeological potential of the submerged landscape, including geological structure, palaeoenvironment, and sea-level change. Swath bathymetry, seismic and subbottom profiling data, side scan sonar imaging and sediment coring indicate that the flat areas belonging to the 70–90 m deep shelf may have developed as part of an erosive marine terrace during the latter part of MIS 3, between 30 and 45 ka BP. A second terrace lying at 115–120 m water-depth is associated with MIS 2, whereas a third one, mapped at about 40 m water-depth, may correspond to the MIS 5.1 period, 80–85 ka BP. Extensional tectonics, possibly driven by basin-ward flow of underlying Miocene evaporites below the shelf, is responsible for the rupturing of the latter along NW–SE trending faults. The resulting fault-bounded blocks, which are composed of Plio-Quaternary rocks, were dragged and drifted away from the shelf edge to create isolated flat-topped ridges surrounded by steep slopes and troughs. The largest part of the shelf along with the 90 m deep, flat tops of the ridges were exposed when the sea-level was at 115–120 m bpsl (below present sea

level) during the Last Glacial Maximum (LGM). This geomorphological configuration may also be valid for the previous low sea-level period, 140 ka BP (MIS 6). Shallow and deep depressions and valleys on the main terrace of the shelf, which formed by solution of evaporite diapirs or domes, were permanent or ephemeral lakes when the shelf was exposed during MIS 2. Similar lakes possibly formed in the many deep sinkholes which occur on the available hydrographic charts along the 120 km wide and several-hundred-km long Farasan shelf. Finally, the presence of valleys and canyons on the seafloor of the survey areas indicates erosion of the shelf under subaerial conditions due to surface water-flow.

1 Introduction

In this paper we present the results of a marine geological-geophysical survey of the Farasan Islands continental shelf, in the southern Red Sea, SW Saudi Arabia. This is a rare example of a marine geological-geophysical survey informed by joint marine-geoscientific and archaeological thinking with the aim of exploring systematically submerged landscapes in deeper areas of the continental shelf and targeting features of potential archaeological significance in relation to geological structure, palaeoenvironment, and sea-level change (for other examples see Dixon and Monteleone 2014). The Red Sea region is of wide interest and significance both to geoscientists and archaeologists: to geoscientists because it represents an unusual ‘laboratory’ for investigating Pleistocene sea-level change (Lambeck et al. 2011) superimposed on a dynamically changing landscape controlled by rift-tectonics and salt-tectonics (Bosworth et al. 2005); and to archaeologists because it is regarded as one of the primary pathways of dispersal for early human populations expanding out of Africa during the Pleistocene, in which the now-submerged landscape of the extensive continental shelf is believed to have played a key role.

D. Sakellariou (✉) · G. Rousakis · I. Panagiotopoulos · I. Morfis
Hellenic Centre for Marine Research, 19013 Anavyssos, Greece
e-mail: sakell@hcmr.gr

G. N. Bailey
Department of Archaeology, University of York, King’s Manor,
York, YO1 7EP, UK

G. N. Bailey
Arts and Social Sciences, Flinders University, College of
Humanities, GPO Box 2100 Adelaide, SA 500, Australia

This study has developed as an international and interdisciplinary collaboration arising directly out of the SPLASHCOS COST Action (www.splashcos.org; Bailey and Sakellariou 2012) and within the ERC-funded project DISPERSE (Bailey et al. 2012). The main objectives were (i) to understand the underlying Quaternary geology and the role of active geological processes in changing the coastal/submerged landscape; (ii) to reconstruct the broad outlines of the now-submerged landscape and (iii) to identify specific locations where archaeological evidence of past human settlement when sea level was lower than present might have been preserved. This work builds on two strands of earlier investigation, one concerned with the impact of active tectonics on the early landscapes of human evolution (King and Bailey 2006; Bailey and King 2011; Bailey et al. 2011), the other with the impact of sea level change and submerged landscapes on the potential connections between Africa and Arabia and the dispersal of early humans expanding out of Africa during the Pleistocene (Bailey et al. 2007; Lambeck et al. 2011; Bailey et al. 2015).

2 Regional Setting

The Red Sea is the youngest oceanic basin on earth, developed as part of an extensive rift system between the Nubian (African) plate to the west and the Arabian plate to the east. Continental rifting in the southern Red Sea and the Gulf of Aden began 30–24 Ma ago (Purser and Bosence 1999, and references therein; Bosworth et al. 2005, and references therein; Bosworth 2015) (Fig. 1). The principal phase of rift shoulder uplift and rapid syn-rift subsidence along the Red Sea followed shortly after 24 Ma. Extension evolved initially perpendicular to the Red Sea rift axis until approximately 14 Ma, when the Aqaba-Levant Transform Fault cut through Sinai and the Levant margin (Bayer et al. 1988) and linked the Red Sea rift with the Bitlis-Zagros convergence zone. Since then, extension across the Red Sea has changed from rift-normal (N60E) to highly oblique (N15E), parallel to the Aqaba-Levant transform fault. During that period, the marine connection with the Mediterranean Sea became restricted and consequently sedimentation in the Red Sea changed from open marine to evaporitic. It was by then, during the Middle to Late Miocene, when massive, up to 2500 m thick evaporites (mainly halite) accumulated on the Red Sea floor (Bosence 1998). The top of the Miocene salt marks a basin-wide unconformity (Hughes and Beydoun 1992; Mitchell et al. 1992), recognized throughout the Red Sea Basin and coincides with the onset of oceanic seafloor spreading in the south-central Red Sea, at latitudes between 15°N and 20°N (Girdler and Styles 1974; Roeser 1975; Searle and Ross 1975; Cochran 1983; LaBreque and Zitellini 1985).

The Red Sea rift is markedly asymmetric. The western (African) margin is narrow and steep, whereas volcanism occurs almost exclusively on the eastern (Arabian) side together with the most significant uplift (Bosence 1998). This asymmetric uplift of the rift shoulders led to the formation of the Great Escarpment, the mountain-front that runs parallel to the Arabian shoreline (Fig. 1). According to Schmidt et al. (1982) the first stage of uplift of the Red Sea Great Escarpment began during Middle Miocene time.

Increased marine water influx through Bab al Mandab in the Early Pliocene (Stoffers and Kuhn 1974; Stoffers and Ross 1977) led to the re-establishment of open marine conditions in the Red Sea (Bosworth et al. 2005). Marine oozes and marginal clastic sediments together with carbonates of Plio-Quaternary age were deposited on top of the Miocene evaporites. Coral reef limestone deposits occur all along the present shorelines and on the shelf and may reach a thickness of up to 300 m, for example, in the Farasan Bank (Mideast Industries Ltd. 1966; Bosence 1998). On the southeastern Red Sea margin, along the littoral zone near Jizan, these deposits are buried under clastic debris derived from erosion of the high rift escarpment.

Salt diapirism began in the Red Sea soon after the widespread deposition of massive halite in the Middle to early Late Miocene. Salt domes reached the surface in many parts of the basin by the end of the Miocene, and most were subsequently buried. A few domes are presently at or very near the seafloor along the Egyptian, Saudi Arabian, and Yemeni margins (Bosworth et al. 2005). Rejuvenation of pre-evaporite extensional fault-systems has stimulated salt mobilization and diapirism in the Red Sea (Purser and Bosence 1999; Hudec and Jackson 2007).

Two shelves have developed along both margins of the Red Sea axial trough, which extend from the shoreline seaward for distances of 30 to more than 100 km. In the southern Red Sea, south of latitude 21°N, where the Red Sea reaches its maximum width of 360 km, both shelves extend for more than 120 km each and are capped by predominantly carbonate sediments (Abou Ouf and El-Shater 1992; Carbone et al. 1998). Two main groups of islands occur in this part of the Red Sea, the Dahlak Islands on the Eritrean shelf and the Farasan Islands on the Arabian shelf. The water depth around the two archipelagos is less than 100 m while the semicircular geometry of the islands and reefs suggests ascending salt domes (Dullo and Montaggioni 1998).

Pleistocene shallow marine reefal limestones, deformed by salt diapirism, form the bedrock of the Farasan Islands (Bantan 1999). The uplift of the Farasan Islands was probably initiated by differential loading of Miocene salt, triggered by tectonic stretching of the overburden during the regional extension of the Red Sea rift. The islands themselves comprise more or less a reef-flat with faulting and uplift strongly influenced by salt diapirism (Dullo and

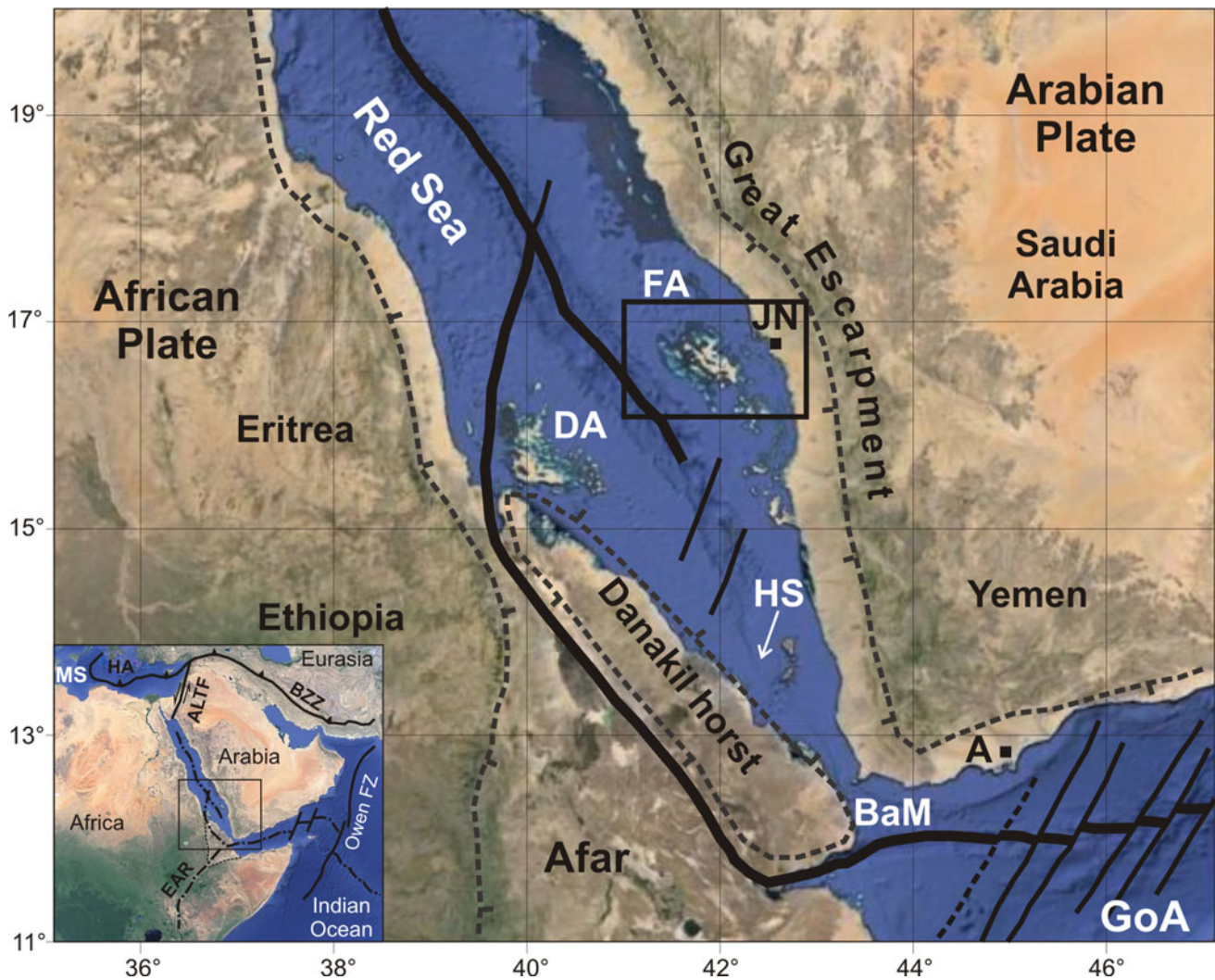


Fig. 1 Google Earth image of the southern Red Sea-west Gulf of Aden with major geodynamic elements modified after Bosworth et al. (2005) showing locations mentioned in the text. A: Aden; BaM: Bab al Mandab Strait; DA: Dahlak Islands; FA: Farasan Islands; GoA: Gulf of Aden; HS: Hanish Sill; JN: Jizan. The black box marks the area shown in Fig. 2

Montaggioni 1998). The tectonic pattern exhibits graben and horst structures developed parallel to the Red Sea trough. Therefore, salt diapirism has created not only dome-like structures but also NW–SE salt walls. The exposed reef limestones are mainly of Eemian age (MIS 5.5, 125 ka BP) and occur at an elevation not higher than 15 m above present sea-level (see Inglis et al., this volume). They are underlain by marly limestones onlapping gypsum and anhydrite domes (Dabbagh et al. 1984; Bantan 1999).

3 Sea-Levels, Palaeogeography and Submerged Landscapes

The MIS 5.5 reef-terrace marks a very prominent and widespread palaeoshoreline at elevations of up to 20 m along the present Red Sea shoreline (Dullo and Montaggioni

1998). Older high-stand terraces, particularly the MIS 7.1 (206 ka BP) and 9.3 (310 ka BP) ones are around 15 m and 30 m above present sea-level (Dullo 1990). On the submerged shelf, three prominent submarine terraces at –20 m, –60 m and –90 m have been recognized in various areas off the Red Sea coasts. The –20 m terrace has been attributed to MIS 5.2 (90 ka BP) and the –60 m terrace formed during MIS 4.2 (64 ka BP) (Gvirtzman 1994). For the most prominent, –90 m deep, terrace, Dullo and Montaggioni (1998) suggested a MIS 3 age, 28–37 ka BP, in accordance with observations in the Indian Ocean by Dullo et al. (1997).

Analyses of sediment cores from the Red Sea floor have shown that it has been open to the Indian Ocean throughout the last 500,000 years at least (Rohling et al. 1998, 2009; Siddall et al. 2004). Palaeosea-level modelling and shoreline reconstructions by Lambeck et al. (2011) confirm that the Red Sea has remained connected with the Gulf of Aden

throughout the last 400,000 years, albeit the cross-sectional areas at times of glacial maxima were about 2% of that today. The minimum channel widths (less than 4 km) connecting the Red Sea to the Gulf of Aden during lowstands occur south of the Hanish Sill (Fig. 1) and remain narrow for as long as local sea levels are below -50 m.

Phylogenetic analyses and interpretations are in favour of the hypothesis that Anatomically Modern Humans originating in East Africa dispersed rapidly about 60,000 years ago across the southern end of the Red Sea to the Arabian Peninsula (Walter et al. 2000; Macaulay et al. 2005; Mellars 2006; but see Bailey et al., this volume). New dates for Stone Age sites in the Arabian Peninsula indicate the presence of humans already since at least 130,000 BP (Petraglia and Rose 2009; Armitage et al. 2011; Petraglia et al. 2011; Rose et al. 2011; Delagnes et al. 2012). Whether the archaeological material at these sites was deposited by Anatomically Modern Humans or not is unclear, but in any case, there is now known to be much earlier archaeological material in the Arabian Peninsula most probably associated with archaic hominin species (Bailey et al., this volume; Petraglia et al., this volume). At any rate, the available sea-level and shoreline reconstructions for the Upper Pleistocene and the Holocene show that the sea channel between the Bab al Mandab Strait and the Hanish Sill remained open throughout this period. Hence, migration from Africa to Arabia across the southern Red Sea would have required sea crossings. However, according to Lambeck et al. (2011), suitable periods for crossing occurred for long periods at times of sea level lowstands, involving sea crossings of no more than 4 km.

Continental shelves, now submerged below the present sea level, should have offered relatively mild climate conditions compared to cold or arid hinterlands during low sea level periods (Bailey and Flemming 2008). In addition, the coastal oasis hypothesis, proposed by Faure et al. (2002), suggests that as sea level dropped, the water from underground springs would have found an easier exit onto the adjacent coastal areas, creating a well-watered coastal lowland—or at any rate coastal oases—potentially attractive to plant and animal life during glacial periods precisely over the time range when overall climatic conditions were becoming drier in the adjacent hinterland.

Within the context described above, the aim of this paper is to present new geological (tectonic, sedimentological) and geomorphological data from the continental shelf of the Farasan Islands, to produce palaeogeographic reconstructions of Pleistocene lowstands and to highlight specific palaeomorphological features which might have been exploited by prehistoric humans.

4 Survey Strategy, Materials and Methods

The continental shelf around the Farasan Archipelago is several hundred kilometres long and over 120 km wide. During the 14 days of the DISPERSE-Farasan cruise aboard R/V Aegaeo, it was necessary to focus on relatively small areas from which to draw conclusions applicable to wider areas of the continental shelf. Two areas were surveyed.

Farasan 1 area (Figs. 2 and 3) is located on the outer edge of the shelf and offers the opportunity to (i) map precisely the seafloor relief, (ii) study the shallow geological structure and the role of faulting and diapirism in the shaping of the shelf edge and the continental slope, (iii) study sedimentary environments and retrieve sediment cores from the outer shelf and the slopes, (iv) map low sea-level palaeoshorelines, particularly the LGM shoreline, and (v) assess hydrogeological conditions and predict possible locations of water points on the outer shelf, particularly springs or spring lines, often located at the foot of low cliffs and fault scarps.

Farasan 2 area (Figs. 2 and 4) is located on the inner shelf, between the Farasan Islands and the Arabian shoreline. The available bathymetric data (GEBCO, International Chart Series Sheet 157, UK Hydrographic Office) show a prominent, NW–SE trending valley, parallel to the main rift axis and a complex topography that appears to drain into a >200 m deep, circular basin, possibly formed by solution or withdrawal of underlying evaporites. The latter could have been freshwater-filled when sea level was low, and may contain a sediment sequence showing the transition from marine to lacustrine conditions as related to changing sea levels in the Upper Quaternary. Along with the objectives already mentioned for the previous study area, Farasan 2 area offers the opportunity to understand the role, character and sedimentation of the deep, circular, sinkholes and reconstruct the submerged landscape of the inner Farasan continental shelf during low sea-level periods.

In addition to the two areas above (Farasan 1 and Farasan 2), two seismic transects (Transect 1 and Transect 2) were shot by using the airgun seismic profiler (Fig. 2).

The marine survey in both areas included a wide variety of geological and geophysical techniques (Figs. 3 and 4): (1) Multi-beam bathymetry with two hull-mounted systems (20 kHz and 180 kHz), (2) Airgun 10ci single channel seismic reflection profiling, (3) High-resolution sub-bottom profiling with a 3.5 kHz pinger, (4) Deep-towed, 110/410 kHz frequency, digital side scan sonar, (5) 3–5 m long gravity coring, (6) $40 \times 40 \times 60$ cm box coring, and (7) ROV dives to visually inspect sites selected from bathymetric, side scan sonar and seismic data.

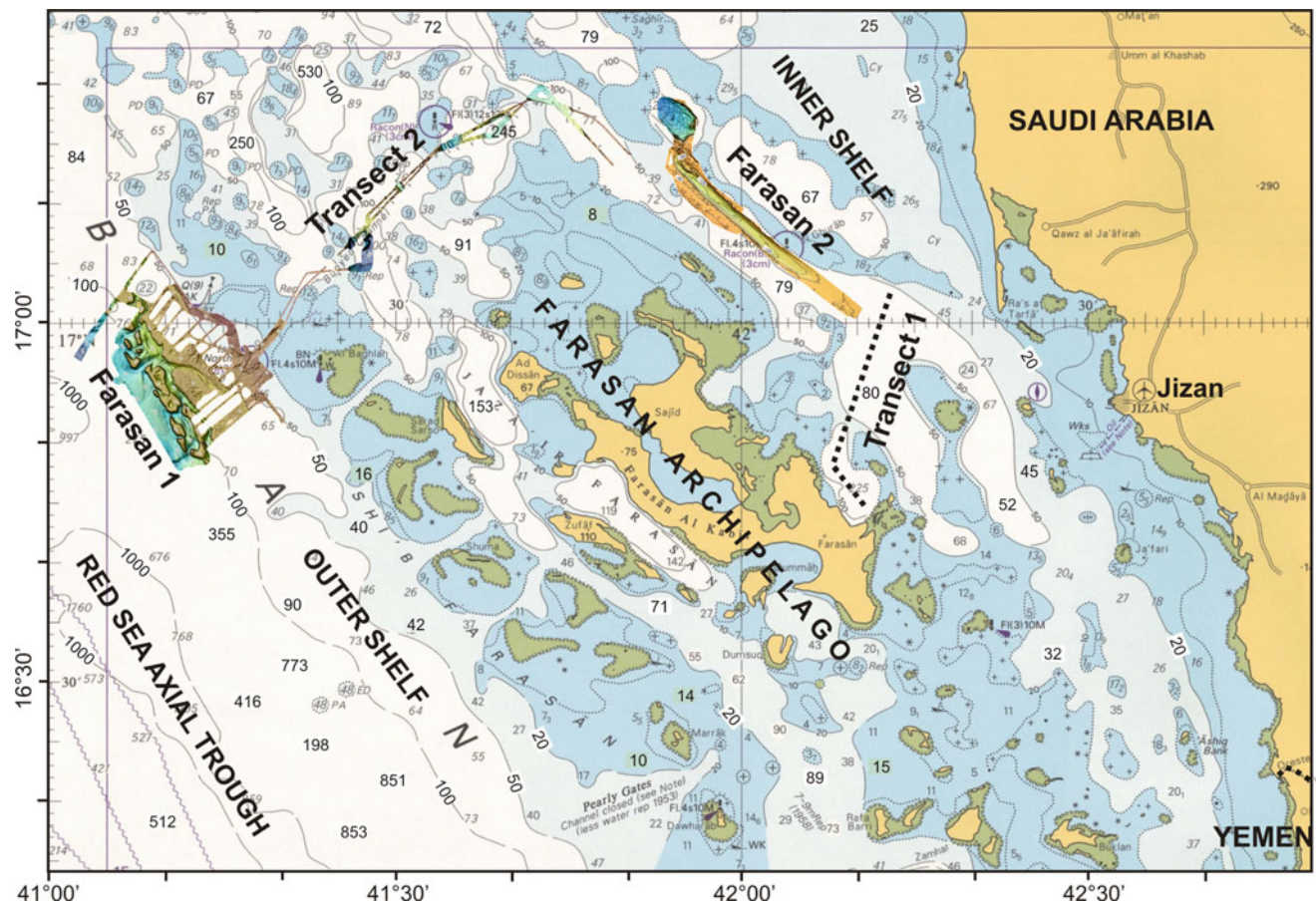


Fig. 2 Extract from the International Chart Series, UK Hydrographic Office Sheet 157, showing the bathymetry of the Farasan Islands continental shelf and the surveyed areas FARASAN 1 and FARASAN 2 during the DISPERSE-Farasan cruise aboard R/V Aegaeo

In total, about 500 km² of the seafloor was mapped with the multi-beam echosounder systems, 170 nautical miles of airgun seismic reflection profiles, 250 nautical miles of 3.5 kHz sub-bottom profiles and 140 nautical miles (260 km) of side-scan sonar lines were acquired. Finally, 18 gravity cores and 2 box-cores were recovered and 5 ROV dives were accomplished.

5 Outer Shelf

5.1 Seafloor Morphology

The most prominent morphological feature of the surveyed outer Farasan shelf is a flat terrace dipping gently toward the axis of the Red Sea, at depths ranging between 70 m landward and 85–90 m toward the shelf edge (Figs. 5 and 9). It corresponds to the 90 m deep terrace widely observed in the Red Sea, which, in accordance with observations in the Indian Ocean (Dullo et al. 1997) has been correlated by Dullo and Montaggioni (1998) with MIS 3, at 28–37 ka

BP. A second terrace, lying at about 40 m depth, has been mapped along the landward edge of the survey area (Fig. 5a). It is separated from the main, deeper terrace by steep slopes locally 30–40 m high (Figs. 5 and 9). A third, narrow terrace occurs off the shelf edge, at about 115–120 m on the steep slopes of the shelf edge and around the flat-topped highs (Figs. 5 and 9). Its width does not exceed a few hundred metres.

Numerous, up to about 20 m high, mostly circular mounds of different sizes occur on the main terrace. They represent coral reefs that have developed following the sea level rise after the LGM (Dullo and Montaggioni 1998). Two valleys incise the flat, 70–90 m terrace (Fig. 3). The first one, at the northern end of the survey area, has developed along the foot of the slope in front of the –40 m terrace (Fig. 5a). Its floor is at about 80 m depth and becomes deeper and wider toward the NW. The second, more prominent valley runs from southeast to northwest in the central part of the survey area (Fig. 5b). The depth of the valley floor increases gradually toward the northwest from about 80–85 m to over 140 m at the outflow to the deep trough off the shelf. Shallow

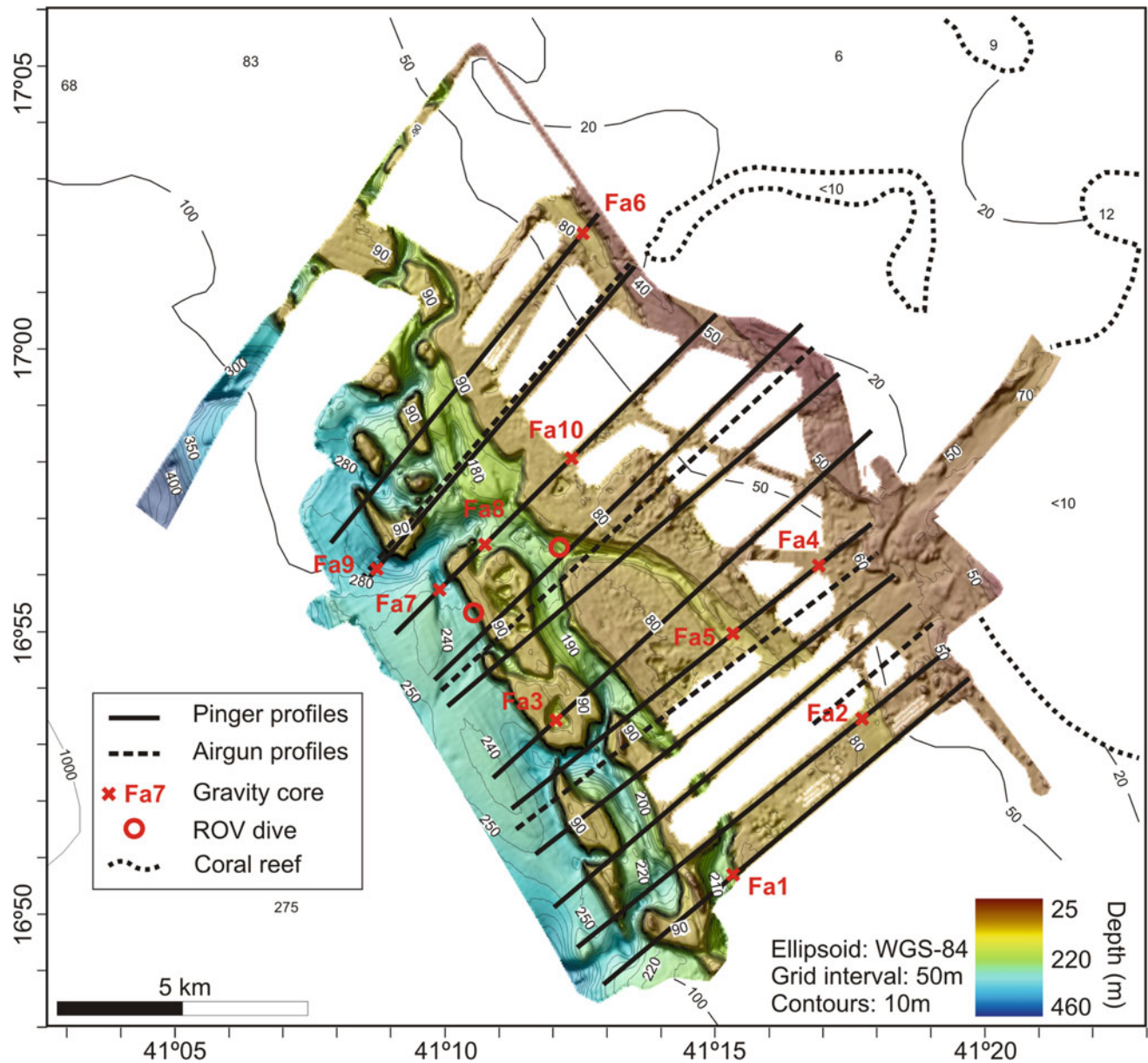


Fig. 3 Survey area FARASAN I on the outer shelf of the Farasan Islands with location of seismic and pinger profiles, side scan sonar tracklines (same as pinger profiles), sediment coring sites and ROV dives. Background: International Chart Series, UK Hydrographic Office Sheet 157 “Masamirrit to Bab el Mandab”, scale 1:750.000 at 20°00’N latitude, depths in metres

isolated depressions occur randomly on the main terrace. They display circular, elongate and irregular shapes and are 10–40 m deeper than the surrounding shelf floor, reaching maximum depths of 140 m water depth.

A 200 m deep, narrow trough aligned SE–NW and bounded by steep margins runs parallel to and off the shelf edge and separates it from a series of shallow, flat-topped ridges or shoals, similar to underwater mesas or drowned, flat-topped islands. The depth of their flat tops below present sea level is about 90 m, very similar to the depth of the shelf

edge. The slopes all around them are very steep, with slope values exceeding 45°. Towards the SW, the steep slopes pass into the continental slope of the Red Sea which displays smooth morphology. The overall impression from the bathymetry is as if these shallow, flat-topped blocks were initially parts of the shelf, then were cut off from it and somehow drifted laterally toward the SW, giving birth to the narrow troughs behind and in between them. More evidence on the nature and origin of the shallow blocks is provided in the following section.

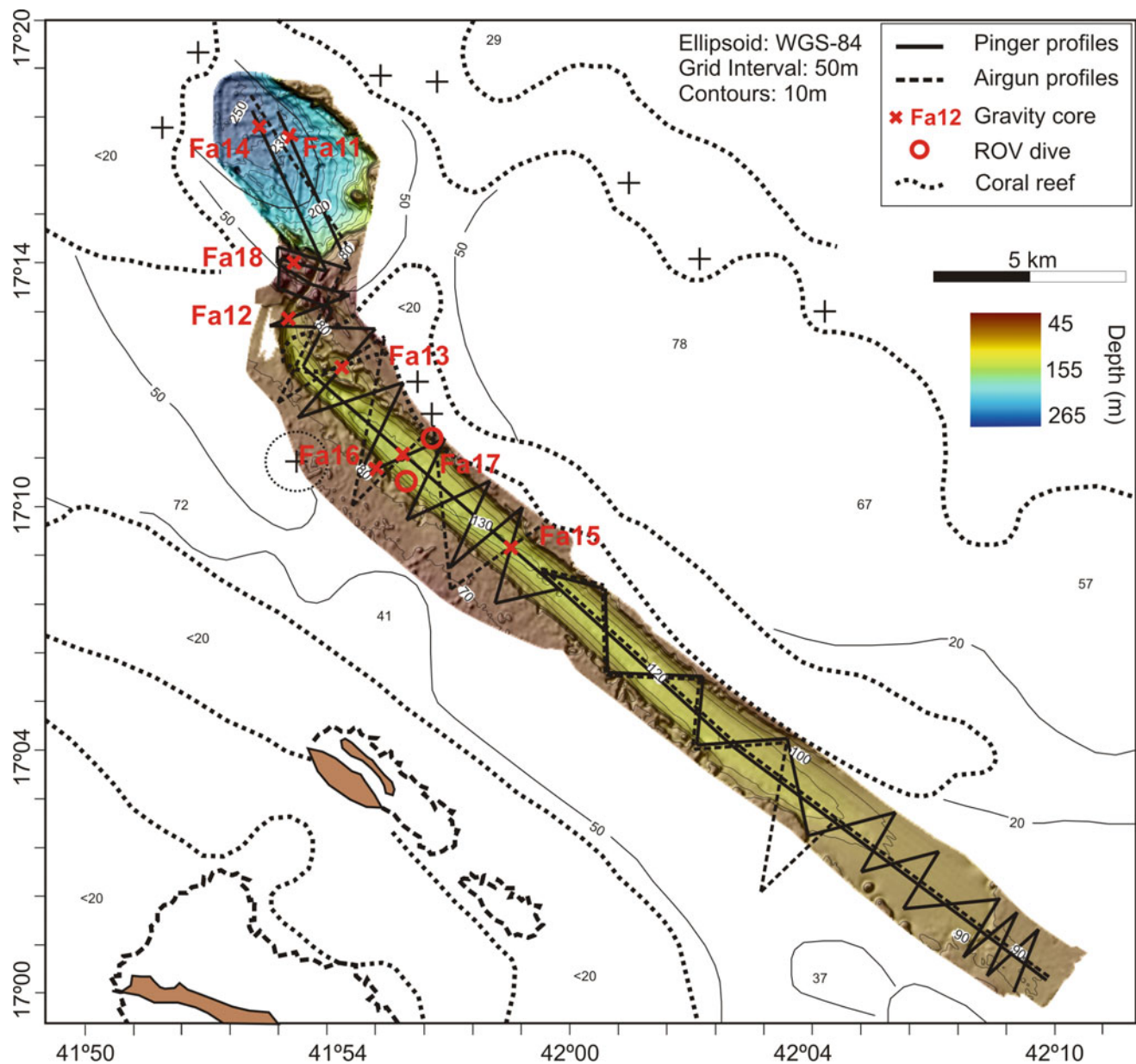


Fig. 4 Survey area FARASAN 2 on the inner shelf of the Farasan Islands with location of seismic and pinger profiles, side scan sonar tracklines (same as pinger profiles), sediment coring sites and ROV dives. Background: International Chart Series UK Hydrographic Office Sheet 157 “Masamirit to Bab el Mandab”, scale 1:750.000 at 20°00' North latitude, depths in metres

5.2 Geological Structure

The interpretation of the seismic profiles shows that the main geomorphological features of the FARASAN 1 survey area have developed under the control of SE–NW running normal faults and fault zones (Figs. 6 and 9). The observed faults do not exceed 10–12 km in length and most of them dip toward the SW. Traces of faults on the seafloor of the main terrace are recognized as morphological scarps and are responsible for the development of valleys incised along the faults on their hanging walls, as is the case for the two valleys

described above and shown in Fig. 5. Total offset produced by the F2 fault is about 35–40 m while the F1 offset is less. Subsidence of the hanging wall of the F2 fault led to the formation of the valley.

The seismic stratigraphic configuration of the shelf shows horizontal packages offset by sub-parallel normal faults (Fig. 6). Strong reflectors mark the boundaries between the six seismostratigraphic packages identified. No angular unconformity can be observed between the older packages 5 and 6. The internal reflectors of package 4 overlap unconformably the top reflector of package 5. Similarly, package 3

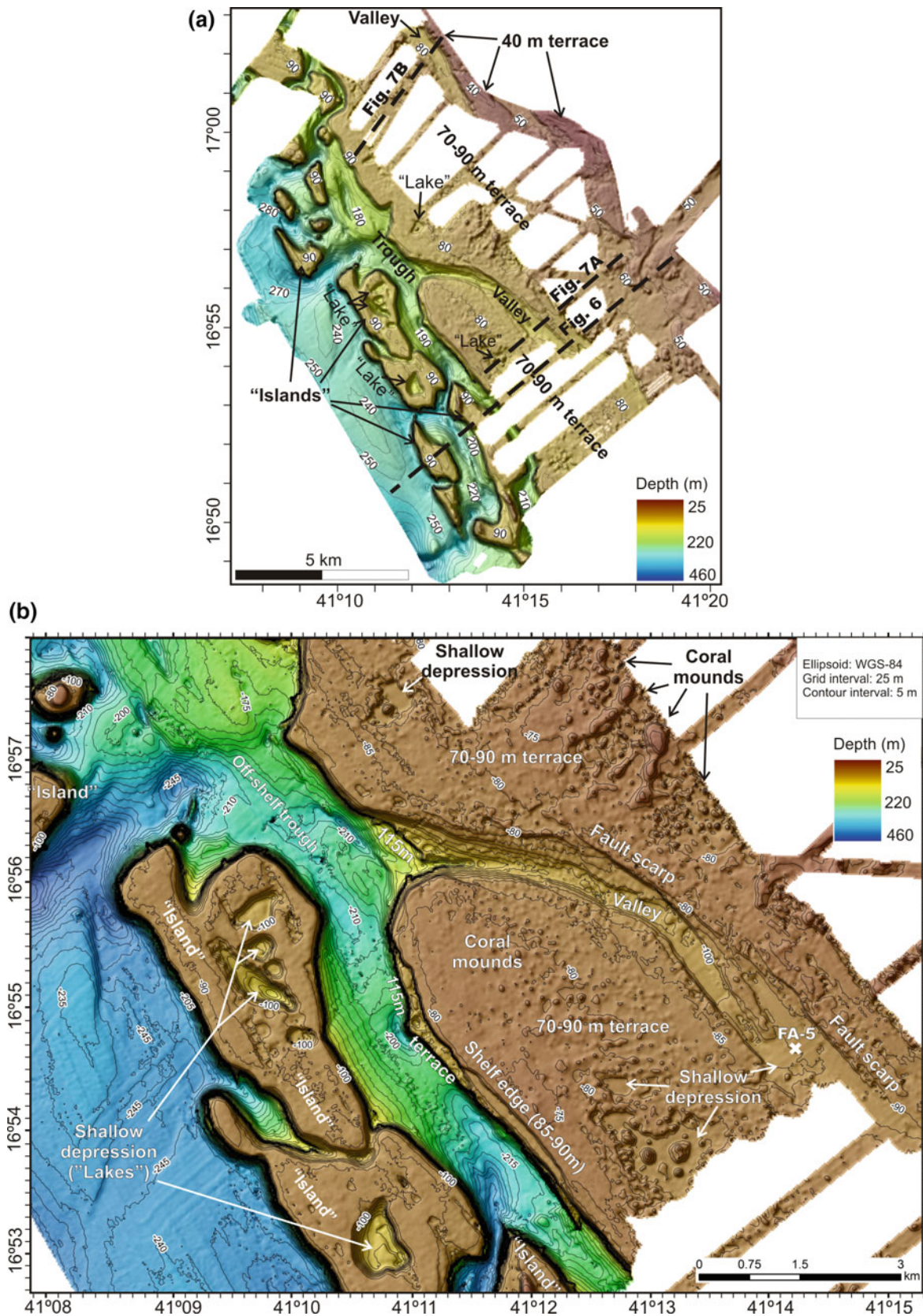


Fig. 5 a Geomorphological elements of FARASAN 1 survey area on the outer shelf. b Enlargement of the central part of the survey area with detailed morphological features and location of core FA-5 shown in Fig. 8

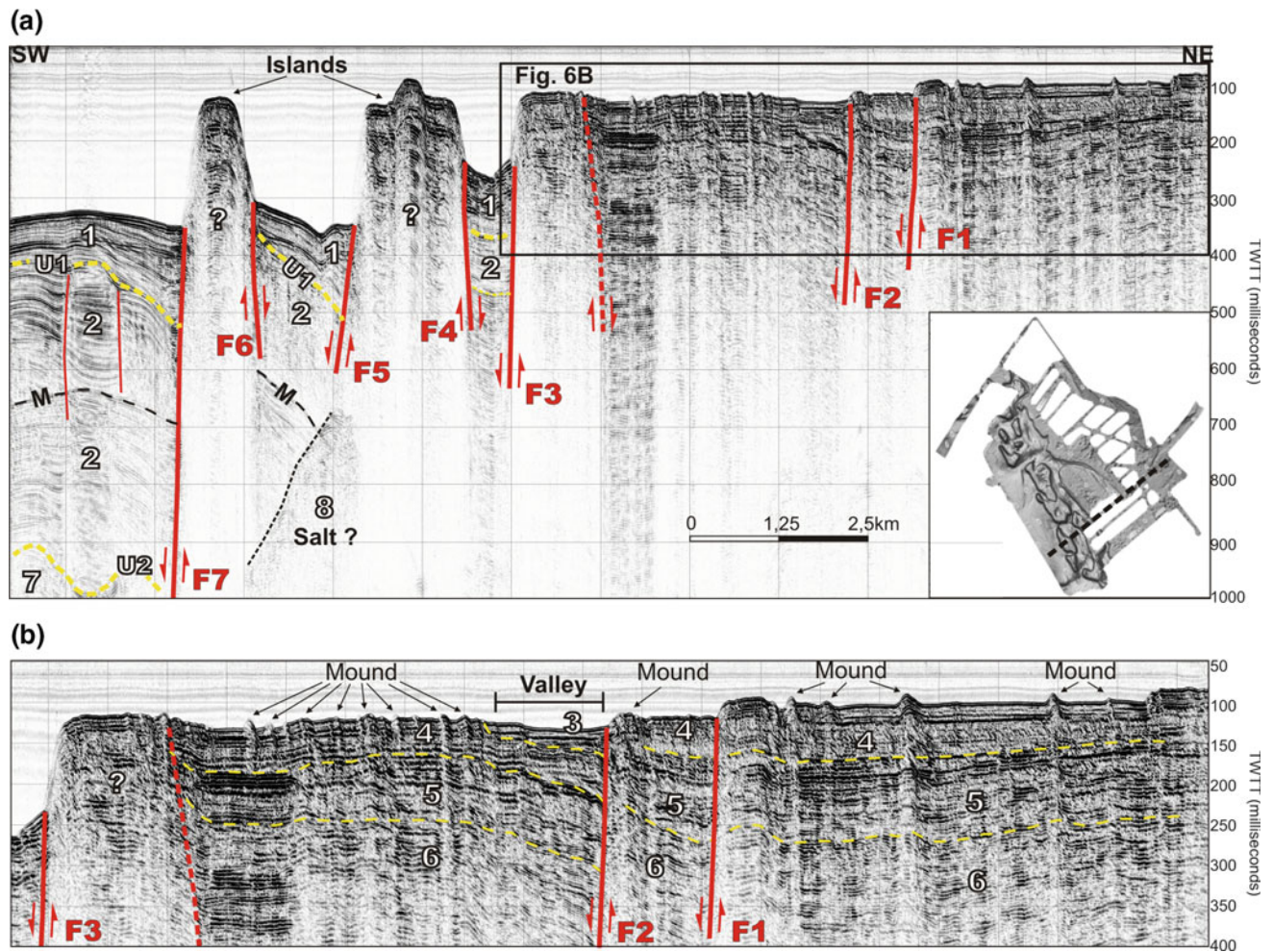


Fig. 6 **a** Airgun 10ci seismic profile across the outer shelf of Farasan Islands. **b** Magnification of the profile on the main shelf. White numbers with black outline correspond to seismostratigraphic packages. U1 and U2 are unconformities. Red numbers with black outline correspond to individual faults. See text for further explanation. M: multiple. Location of the profile in inset and in Fig. 5a. Vertical exaggeration $\times 10$

lies unconformably over the top reflector of package 4. The seismostratigraphic package 3 occurs only locally, in the small depression in the hanging wall of one of the SW-facing normal faults. This depression coincides with the SE–NW oriented valley that runs through the central part of the survey area (Fig. 5b).

The seismostratigraphic package 3, with a maximum thickness of about 30 ms (roughly 22–23 m), occurs only locally, in the shallow depressions or valleys of the shelf. It represents the youngest deposit on the shelf, probably of Upper Quaternary (Holocene and Uppermost Pleistocene) age. Packages 4, 5 and 6 are characterized by parallel, continuous, locally undulating reflectors and may correspond to the Pleistocene shallow marine reefal limestone, which forms the bedrock of the Farasan Islands (Bantan 1999).

The shelf terminates sharply toward the SW and is followed by two shallow, flat-topped blocks (Islands on Fig. 6a) which are separated from each other and from the shelf by deep, narrow, fault-bounded troughs (Fig. 6a). Although the seismic stratigraphy of the ridges is poorly imaged due to the very irregular topography of their tops, internal sub-parallel reflectors are recognized and it is supposed that the sedimentary sequence of their substrate is comparable to the one described below the main shelf. Despite the faults separating them, no vertical offset can be measured between the main shelf and the shallow blocks. The narrow troughs formed between the shallow blocks and the shelf's edge host sedimentary deposits exceeding 150 m in thickness. The seismic units 1 and 2, which fill the troughs, are characterized by parallel and continuous reflectors and are separated from each other by an angular unconformity U1.

Thick sedimentary deposits occupy the seafloor substrate southwest of the steep shallow ridges. Seismic unit 1 displays a maximum thickness of about 200 ms (>150 m) next to the marginal fault F7 and covers unconformably unit 2. The latter is >500 ms (>400 m) thick and is separated from the underlying unit 7 by the unconformity U2. Finally, one more seismic unit, unit 8, is observed at depth below the islands. Its chaotic to transparent seismic character may indicate the presence of mobilized salt deposits.

The seismostratigraphic description of the seismic profile and the interpretation of the geological structure of the shelf edge, as described above, strongly indicate that the shallow, flat-topped blocks (islands) off the shelf-edge were initially belonging to the shelf. They were cut off and separated from the shelf due to predominantly NW–SE trending faulting and the subsequent formation of the deep troughs between them. The irregular shape of the blocks, along with the absence of any vertical offset between them and the shelf-edge indicate that the breakup process may not be of purely tectonic origin. There is neither evidence of compression nor any indication of strike slip deformation. Extensional tectonics with normal faulting might be able to offer a solution to their formation but the fact that there is no vertical offset between the ridges and the shelf is against it. A possible explanation can be found in deformation processes related to the underlying Miocene evaporites. Extensive basin-ward salt flow in the form of salt glaciers or namakiers has been observed and documented in the central Red Sea (Augustin et al. 2014; Feldens and Mitchell 2015; Augustin et al., this volume). Alongslope and downslope ridge and trough morphologies have developed on the flow surfaces, parallel to the local seafloor gradient, presumably due to extension of the sedimentary cover or strike-slip movement within the evaporites (Feldens and Mitchell 2015). The morphology of the deep troughs and the flat-topped ridges and shoals mapped off the Farasan islands shelf-edge is very similar to one of the ridges and troughs observed in the central Red Sea. Therefore, it is reasonable to assume that basinward flow of the Miocene evaporites has occurred below the Farasan shelf too. Dragging of the overlying sedimentary cover due to the salt flow underneath has led to breakup and drifting of sedimentary blocks toward the axis of the Red Sea and away from the shelf, leaving space behind them for the formation of the deep troughs. The absence of vertical offset between the blocks and the shelf supports this drifting hypothesis.

5.3 Sedimentation

High resolution subbottom profiles across the outer shelf (Fig. 3) show that the recent Holocene sediment deposition has been very limited. Two profiles from the central

(A1–A2) and the northern (B1–B2) parts of the survey area (Fig. 7) show representative cross sections of the outer shelf. The main terrace on the outer shelf is flat and dips gently southwestward from roughly 70 m landward to 85–90 m seaward. Numerous mounds, up to 20 m high, rise above the flat shelf-floor and give it a unique geomorphological character. The 40 m deep terrace occurs at the northeastern end of A1 profile in Fig. 7.

The largest part of the shelf is free of Holocene sedimentary deposits, and the Quaternary shallow marine sedimentary rocks which outcrop on the Farasan Islands (Bantan 1999) are exposed on the shelf floor. Recent sediments have been observed only in the depressions and valleys on the main terrace. They display a transparent seismic character and their thickness depends on the morphology of the substrate. It ranges from a few decimetres in the shallowest parts of the depressions and valleys to 15–20 m maximum in the deepest parts.

Detailed sedimentological, geochemical and radiometric analyses on the cores retrieved from the shelf are in progress, in collaboration with the Scottish Universities Environmental Research Centre (see Sanderson et al., this volume) and the Saudi Geological Survey. Here we present some basic observations indicating that homogeneous, marine, up to 3 m thick, fine-grained deposits pass downward into coarser sediments. The latter display evidence of lacustrine depositional environments.

Ten cores have been collected from the outer shelf survey area with the objective to unravel the nature of the recent sedimentary deposits and the sedimentation environment. Core FA-5 (Fig. 8) has been taken from the southeastern part of the valley that runs through the central part of the survey area (Fig. 5) and provides insight into the sediments deposited in the depressions of the shelf. The coring site, at the centre of the valley, constitutes a local deep surrounded by shallower depths. The upper part of the core, from 0 cm down to 286 cm below the seafloor, consists of fine, olivine green sand. The physical properties of the sediment remain stable, apart from a decrease in the magnetic susceptibility at 150 cm bsf (below seabed surface). After a 3 cm-thick layer with shell debris at 286–289 cm, all properties show marked changes, including a sharp decrease of the magnetic susceptibility. A gradual change in colour from olivine green to grey occurs between 300 cm and 330 cm bsf while the grain size becomes coarser. Large bivalves and shell fragments occur between 330 cm and 360 cm, while the grain size decreases again below 360 cm until the bottom of the core at 363 cm.

The sedimentological description of FA-5 (see Fig. 5 for location) along with the down-core physical properties indicate a significant change in the depositional environment. The upper part of the core represents homogenous marine sedimentation during the present high-stand period.

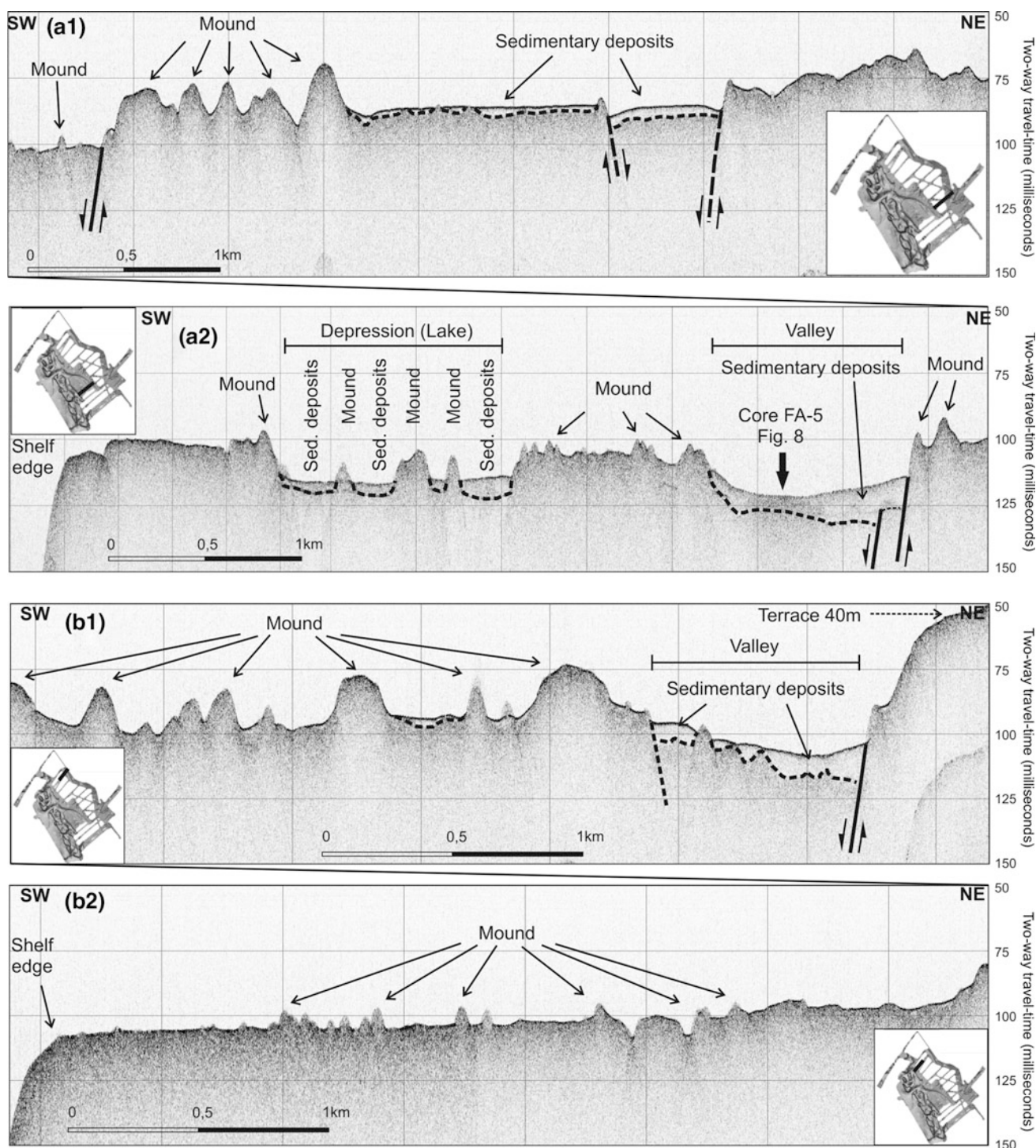


Fig. 7 Two subbottom profiles (3.5 kHz) across the outer shelf of Farasan Islands. A1 and A2 are the two halves of one profile in the central part of the survey area. B1 and B2 are the two halves of a second profile in the northern part of the survey area. Holocene sediments occur only in the depressions of the shelf. Note the numerous mounds rising from the shelf's seafloor. Location of the profiles in Fig. 5a. Vertical exaggeration $\times 20$

The lower part of the core, below 3 m bsf, displays sedimentological evidence of lacustrine environments prevailing in the valley during the last low sea-level stand, when the

shelf was exposed. Significant change of the environmental conditions at the end of the LGM has also been recorded in the sediments deposited off the shelf. Core FA-9 (see

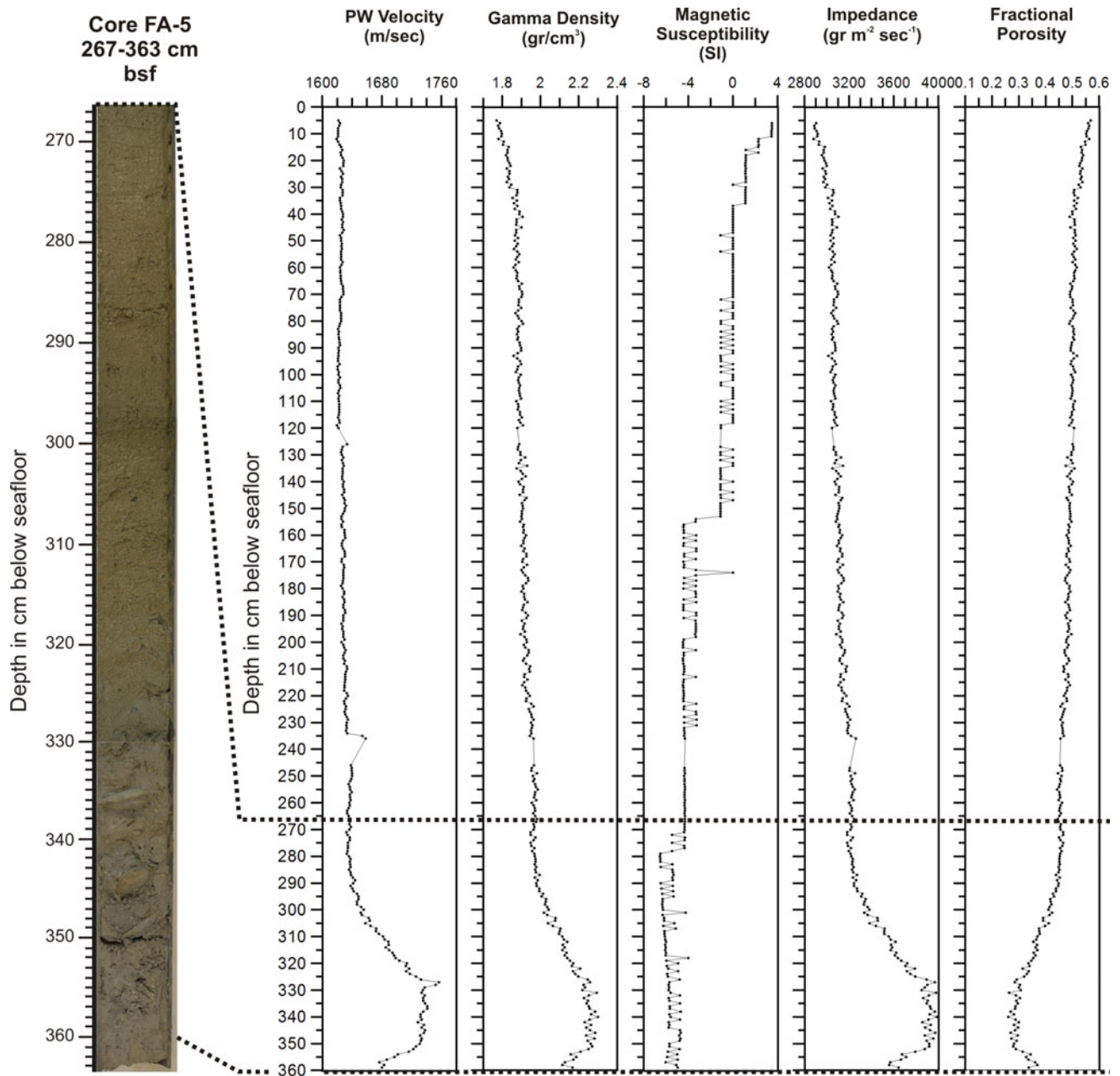


Fig. 8 Physical properties of core FA-5 and photo of the lower part of the core, between 267 and 363 cm below the seafloor. The location of the core (lat: $16^{\circ}54.647'$, long: $41^{\circ}14.237'$, depth 92 m) is shown on the map of Fig. 5b and on the subbottom profile A2 of Fig. 7. Note the gradual change in sediment colour from olive green to grey between 300 cm and 330 cm and the change in the properties below 270 cm

location in Fig. 3) has been retrieved from the margin of the Red Sea basin at 302 m depth, close to the foot of the basin-ward facing slope of one of the “Islands” (Fig. 3). Micropaleontological analyses on the sediments of the core confirm the presence of a major change in the productivity of the Red Sea waters at 130 cm bsf, which is associated with the transition from the Late Glacial to the Holocene periods (see Geraga et al., this volume, for details).

5.4 Outer Shelf Submerged Landscapes and Palaeoshorelines

Integration of the swath bathymetry, seismic and subbottom profiling data and sediment cores presented above reveals the palaeo-geomorphological evolution of the Farasan Islands outer shelf with respect to Upper Quaternary fluctuating sea-level.

Seismic profiling and swath bathymetry data show that the area has been affected by extensive faulting, presumably associated with salt flow in the deeper stratigraphic levels. Dragging and deformation of the overlying Plio-Quaternary deposits due to the flow of the underlying Miocene salt deposits toward the axis of the Red Sea has been well documented in the central Red Sea (Augustin et al. 2014; Feldens and Mitchell 2015; Augustin et al., this volume). Apparently, salt flow occurs below the Farasan Island shelf too and results in the separation of blocks from the edge of the shelf and their drift towards the SW. No significant vertical offset has been observed between the drifted blocks and the shelf. The faults running along the outer shelf display rather limited vertical throws while the shelf remains flat. These are good evidence that vertical tectonics during the Quaternary has been very low.

In the absence of direct chronological constraints, we attempt to estimate the age of the observed underwater terraces indirectly, by comparing their depths with the available sea-level curves for the Red Sea. This comparison can provide realistic hypotheses on the ages of the terraces in particular because vertical tectonics in the area of the Farasan outer shelf is negligible as discussed above. Predicted sea levels in the Red Sea during the LGM, 20,000 years BP, show considerable geographic variability, with relatively low values for the northern (105 m bpsl [below present sea level]) and southern (115 m bpsl) ends and deeper values (130 m bpsl) for the central part (Lambeck et al. 2011). The 115–120 m terrace observed locally along the steep slopes off the shelf edge and around the isolated ridges (“islands”) must have been formed during the LGM and is thus indicative for the position of the LGM shoreline at the latitude of the Farasan Islands (Fig. 9). In that case, the outer shelf, the depth of which does not exceed 90 m, as well as the tops of the isolated ridges off the shelf, were subaerially exposed during the LGM. The shelf was part of a wide, flat coastal plain attached to the Arabian landmass while the tops of the isolated ridges were flat-topped islands separated from each other and from the mainland by narrow and deep channels or troughs. Note that the shape of the LGM islands as outlined by the palaeoshoreline is very similar to the shape of the present islands which form the Farasan Archipelago.

The 70–90 m deep terrace occupies the largest part of the outer shelf. Assuming negligible vertical tectonics in the area, the time of the formation of the terrace can be estimated by comparing its depth with the predicted sea-level curve. The inset diagram in Fig. 9 shows part of the sea-level curve of Rohling et al. (2013) for the Red Sea for the last 150 kyr. The depth of the main terrace coincides with the predicted depth on the curve between 30 ka and 45 ka BP, which is the upper half of MIS 3. According to this curve, the sea-level has fluctuated between 75 m and

85 m bpsl during this period. Similarly, the 40 m deep terrace can be correlated with the period 80–85 ka BP (MIS 5.1) when the sea-level was between 35 m to 45 m bpsl.

Based on the subbottom profiling and the sediment coring data, the small depressions on the main shelf display a dual character: firstly, they constitute the depocentres of the marine sedimentation on the shelf during the post-LGM sea-level rise, and secondly, they hosted the deposition of lacustrine sediments when the shelf was subaerially exposed during the LGM. Consequently, the small and shallow depressions and parts of the valleys on the shelf were lake basins during the LGM (Fig. 9).

6 Inner Shelf

6.1 Seafloor Morphology

The survey area in the inner shelf of the Farasan Islands is characterized by two main morphological features (Fig. 10): a 35 km long, 2–2.5 km wide, up to 130 m deep, SE–NW trending, straight valley and a 250 m deep, ellipsoidal depression in the northern end. The southeastern part of the valley is wider and 90–100 m deep. Toward the NW it becomes narrower and reaches 130 m depth close to its northwestern end, where it turns northward and terminates against a shallower area with irregular morphology. The bottom of the valley is rather flat and is bounded by steep, up to 60 m high slopes (Fig. 10c). On both sides of the valley the seafloor is rather flat, with mean depth around 70 m and with numerous mounds. It corresponds to the 70–90 m terrace on the outer shelf.

A 2 km long, 200 m wide and 85 m deep canyon with steep slopes connects the northernmost tip of the SE–NW trending valley with the southernmost tip of the deep, ellipsoidal depression. The latter, the Deep “Lake” in Fig. 10a, b, is 8.5 km long by 4.5 km wide and 250 m deep with the maximum depths occurring close to its northwestern edge. It is surrounded by very steep slopes, locally steeper than 50–60%, which pass upward to very shallow reefs, not suitable at all for navigation. The shape of this deep and steep depression along with the widespread presence of evaporites and diapirs in the subsurface indicates that it has been formed by the solution of a salt dome or diapir.

The backscatter image on Fig. 10B2 depicts very nicely the differences in the acoustic character of the seafloor. The deep depression displays very low reflectivity, which points to very fine sedimentary deposits and a smooth seafloor. The irregular morphology of the shallow parts coincides with the high backscatter (dark) area where the substrate is expected to be exposed on the seafloor and eroded. Finally, the seafloor in the valley and in the small depression on the

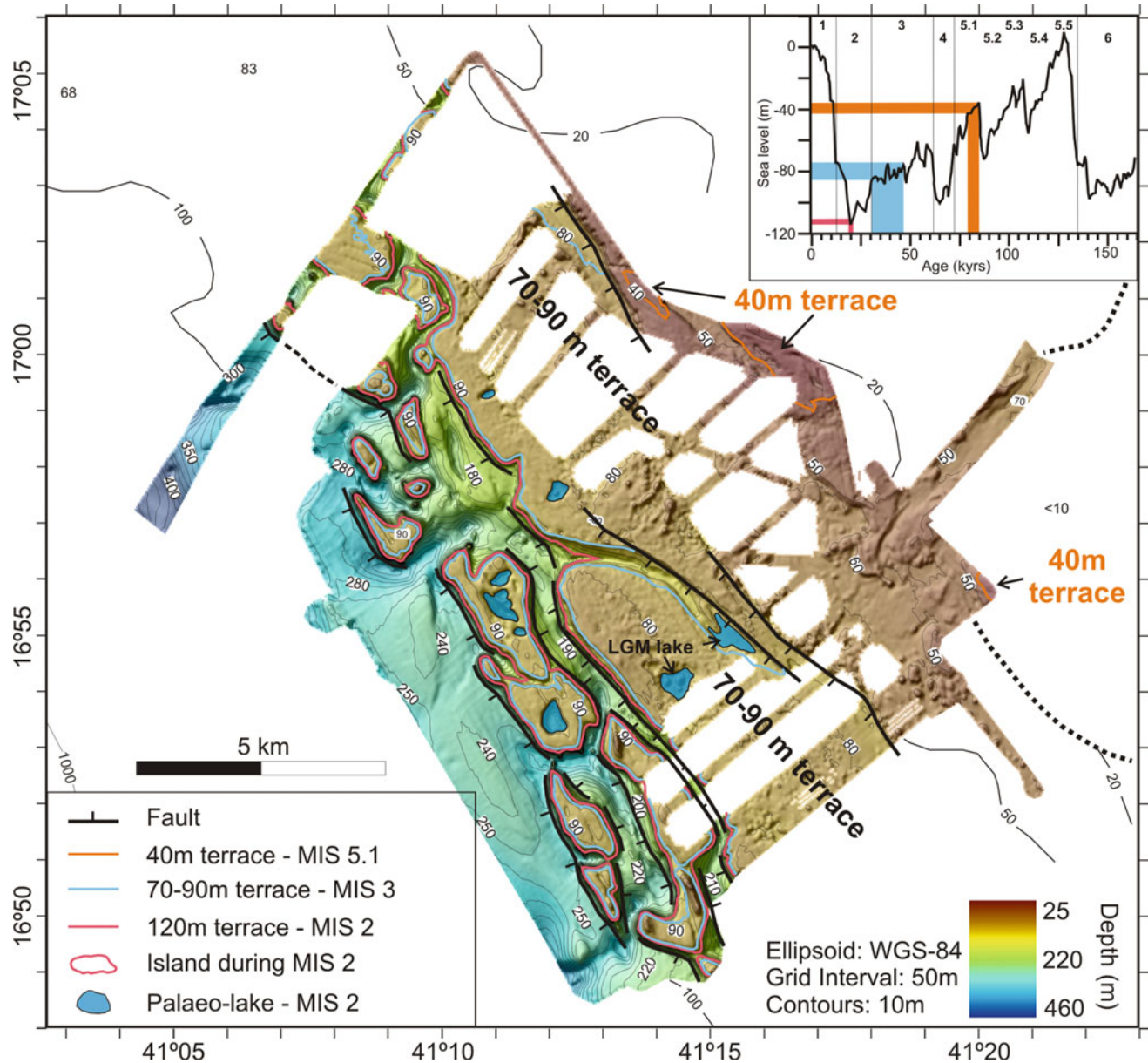


Fig. 9 Shaded bathymetry with tectonic and geomorphological features of the outer shelf. The inset diagram shows the correlation of the three observed underwater terraces (40 m, 70–90 m, 115–120 m) with the sea-level curve of Rohling et al. (2013) for the Red Sea

northern side of it display moderate to low reflectivity, which is indicative for the deposition of relatively coarser sediments with respect to the ones in the deep depression. The slopes along the two sides of the valley are in general linear (Fig. 10c). In a closer view, they display high morphological irregularity, with many invaginations and embayments, which are probably evidence for subaerial erosion on the flanks of the valley. The lower parts of the flanks, deeper than 100 m, dip at an angle of roughly 5% toward the axis of the valley. The upper parts, between

100 m and 70 m, are significantly steeper and display slope values of 25–30%.

6.2 Geological Structure and Sedimentation

The seismic and subbottom profiles shown on Figs. 11 and 13 provide insight into the geological structure and sediment accumulation on the Farasan Islands inner shelf, in particular in the long, straight valley and deep depression.

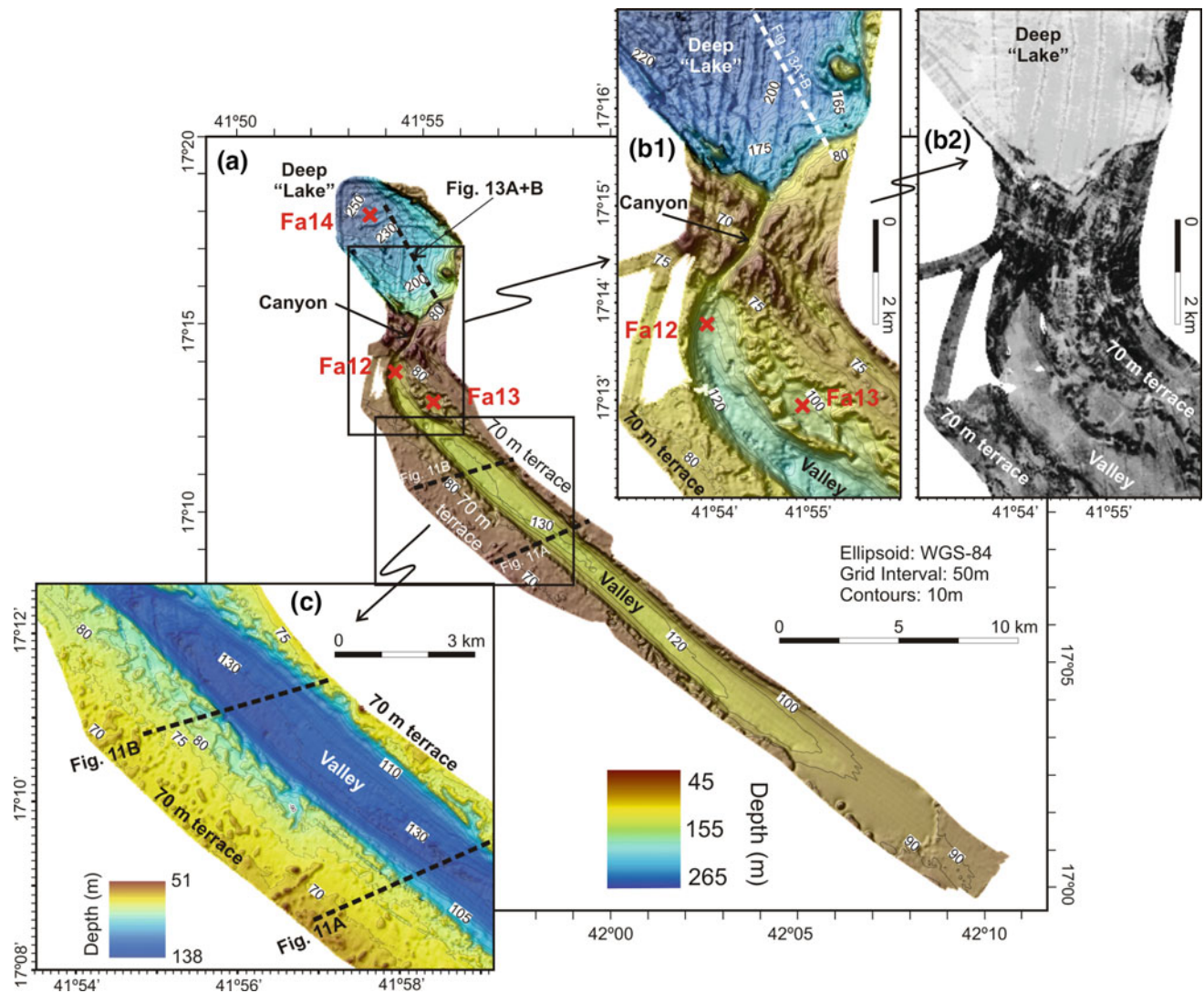


Fig. 10 a Shaded bathymetry and main morphological elements of Farasan 2 survey area on the inner continental shelf. **b1** Detailed bathymetry of the northern part of the Farasan 2 area. Note the canyon connecting the valley with the deep depression. **b2** Backscatter image of the same area as in B. Note the large variability in seafloor reflectivity. **c** Detailed bathymetry of the northern part of the valley. Note the irregular morphological configuration of the two slopes of the valley. Location of the profiles of Fig. 11 are shown on C. Location of the profiles in Figs. 11 and 13 are shown on a and c. Locations of cores FA-12 (Fig. 12) and FA-14 (Fig. 14) are shown on A

The substrate of the inner shelf (Fig. 11a) displays a stratigraphic succession that is very similar to the one observed below the outer shelf (Fig. 6b). The seismostratigraphic package 3 is the youngest deposit on the inner shelf, and occurs only in the valley with a maximum thickness of 20 ms (roughly 15 m) and must have been deposited during the Upper Quaternary (Holocene and Uppermost Pleistocene). The packages 4, 5 and 6 occur below the valley and the shelf south of it; they are characterized by parallel, continuous, locally undulating reflectors and may correspond to the Pleistocene shallow marine reefal limestone, which forms the bedrock on the Farasan Islands (Bantan 1999). Two opposite, normal faults run along the walls of

the valley and are responsible for its formation and subsidence. The total vertical offset of the southern fault is 70 m, as inferred from the depth difference of the bottom of the seismic package 4 at both sides of the fault. The seismic stratigraphy on the foot wall of the northern fault is different from the one below the valley. No stratigraphic correlation can be made between seismic reflectors on both sides of the fault. Thus, the offset produced by this fault cannot be measured in the same way as for the southern fault. Therefore, using the seafloor as a marker, we suggest that the vertical offset of the northern fault is comparable to that of the southern fault, and that the valley has been formed within a symmetric graben.

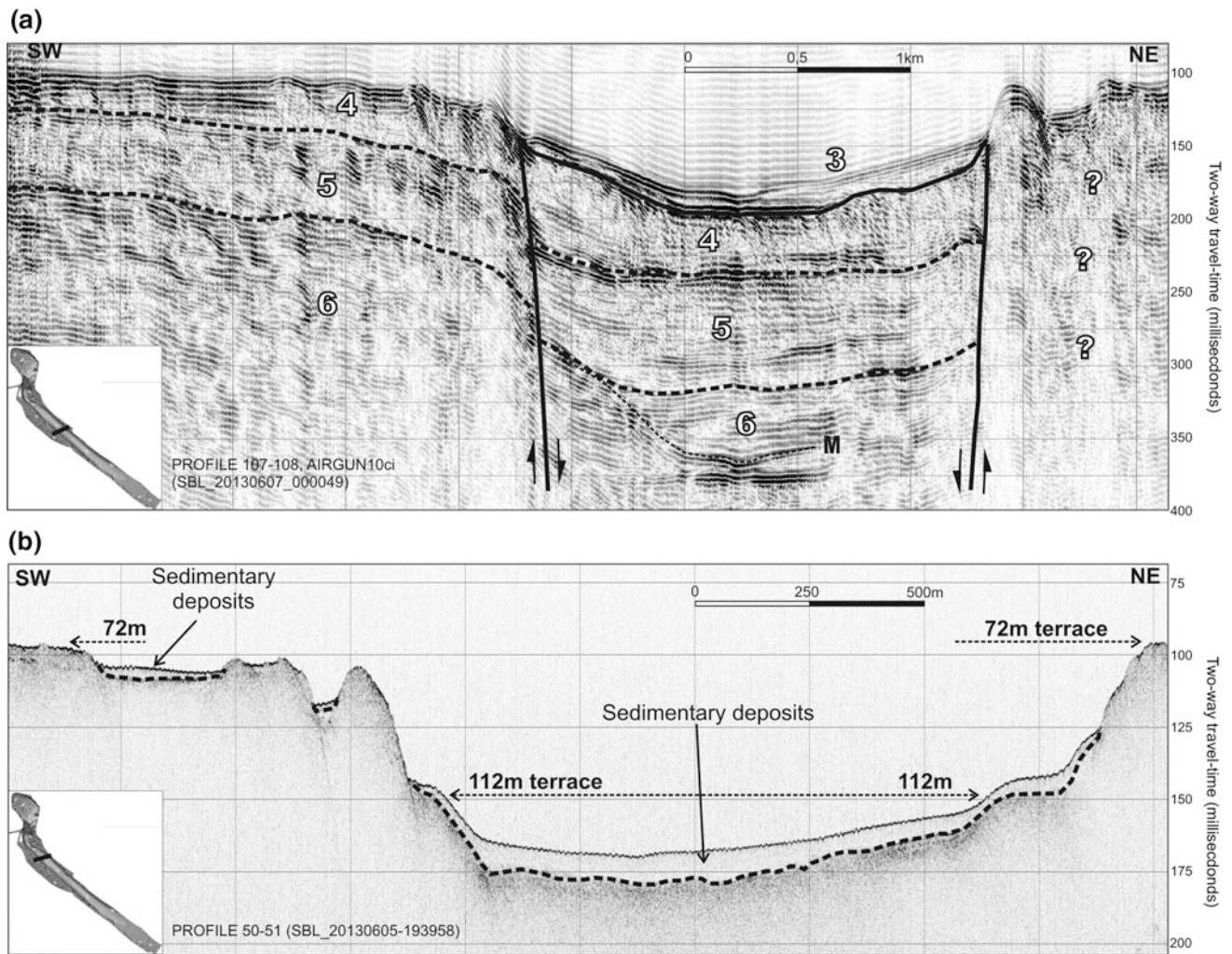


Fig. 11 **a** Airgun 10ci seismic reflection profile across the valley in the inner shelf of Farasan 2 survey area. Vertical exaggeration $\times 10$. **b** High resolution subbottom profile across the same valley. Vertical exaggeration $\times 20$. The locations of both profiles are shown on Fig. 10

The subbottom profile in Fig. 11b displays a higher resolution image of the stratigraphy across the valley. Recent sediments with transparent acoustic character have been deposited in the valley and cover the acoustic basement of the area. The thickness of the acoustically transparent deposits does not exceed 10 ms (7–8 m roughly) which is about half of the thickness of the seismostratigraphic package 3, that is, the topmost package observed on the airgun profile (Fig. 11a) in the valley. The top of the acoustic basement, below the transparent deposits, displays an erosional terrace at 112 m on both sides of the valley (Fig. 11b). This terrace has formed due to the activity of water when this area was exposed and before the deposition of the transparent sediments. The valley has been incised on a flat plain which now forms the shelf seafloor at about 70 m depth. There is no evidence of any morphological element connecting the valley with the LGM sea, the shoreline of

which has been identified at 115–120 m in the outer shelf survey area. Consequently, the 112 m terrace in the valley could not be formed as a marine one. Instead, it may constitute good evidence that the valley was a lake with water level at this position during the LGM.

The sediment core FA-12 (Fig. 12) retrieved from the northern end of the valley at 105 m depth bpsl confirms a major change of the depositional environment downcore. The upper part of the core, from 0 cm down to 90 cm bsf, consists of medium to coarse, olivine green sand with bivalves and shell fragments. The sediment colour changes at 90 cm bsf from olive green above to bluish gray below along with a gradual fining of the grain size to mud with some thin layers of sand. Similarly, a major change in the physical properties of the sediment, including a significant increase in magnetic susceptibility, occurs at 90 cm bsf. The sedimentological description of FA-12 along with the down-core physical properties indicate

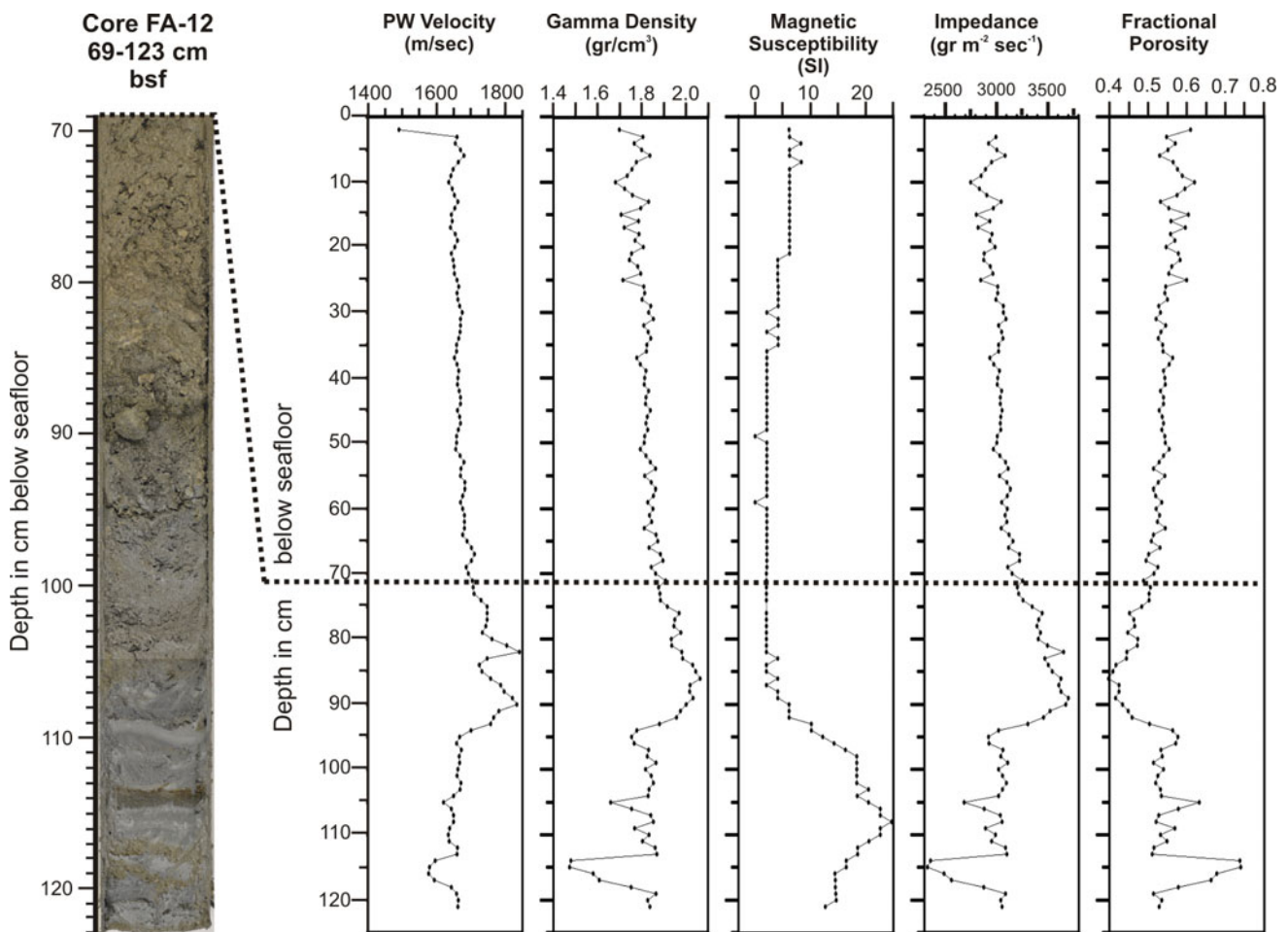


Fig. 12 Physical properties of core FA-12 and photograph of the lower part of the core, between 69 and 123 cm below the seafloor. The location of the core (lat: 17°13.719', long: 41°54.070', depth 105 m) is shown on Fig. 10. Note the change in sediment colour from olive green to grey at 90 cm bsf which coincides with the change in the properties at the same depth

a significant change in the depositional environment at 90 cm bsf. As with core FA-5 from the outer shelf (Fig. 8), the upper part of core FA-12 represents homogeneous marine sedimentation during the present high-stand period. The lower part, below 90 cm bsf, displays evidence of a lacustrine sedimentary environment prevailing in the valley from which the core has been recovered, during the last low sea-level stand, when the shelf was exposed. The sediment core FA-13 was retrieved from 102 m depth within a small depression at the northern margin of the valley (Fig. 10a, b). Sedimentological, geochemical and radiometric data from this core display a stratigraphic pattern very similar to the one observed in core FA-12 and confirm that the change in the sedimentary environment is associated with the post-LGM sea-level rise (see Sanderson et al., this volume, for details).

The deep depression at the northern part of the Farasan 2 survey area is the second major feature of the inner shelf

(Fig. 10a, b). This 250 m deep depression hosts sedimentary deposits more than 600 ms (roughly 500 m) thick (Fig. 13a). The uppermost, less than 20 ms thin, seismostratigraphic package A drapes the irregular top of package B. The high-resolution profile of Fig. 13b provides a precise image of the stratigraphic architecture of the uppermost sedimentary deposits. The seismostratigraphic package A displays a rather transparent character with one layered horizon in the middle. It has been deposited on top of package B, on a fairly irregular reflector that marks the interface between packages A (transparent) and B (acoustic basement on the sub-bottom profile). The latter, with a maximum thickness of 100 ms (75–80 m) at the north-western edge of the depression (Fig. 13a), displays a rather chaotic seismic character with few discontinuous, strong, parallel, internal reflectors. Two seismostratigraphic packages, C and D, are separated from each other by an angular

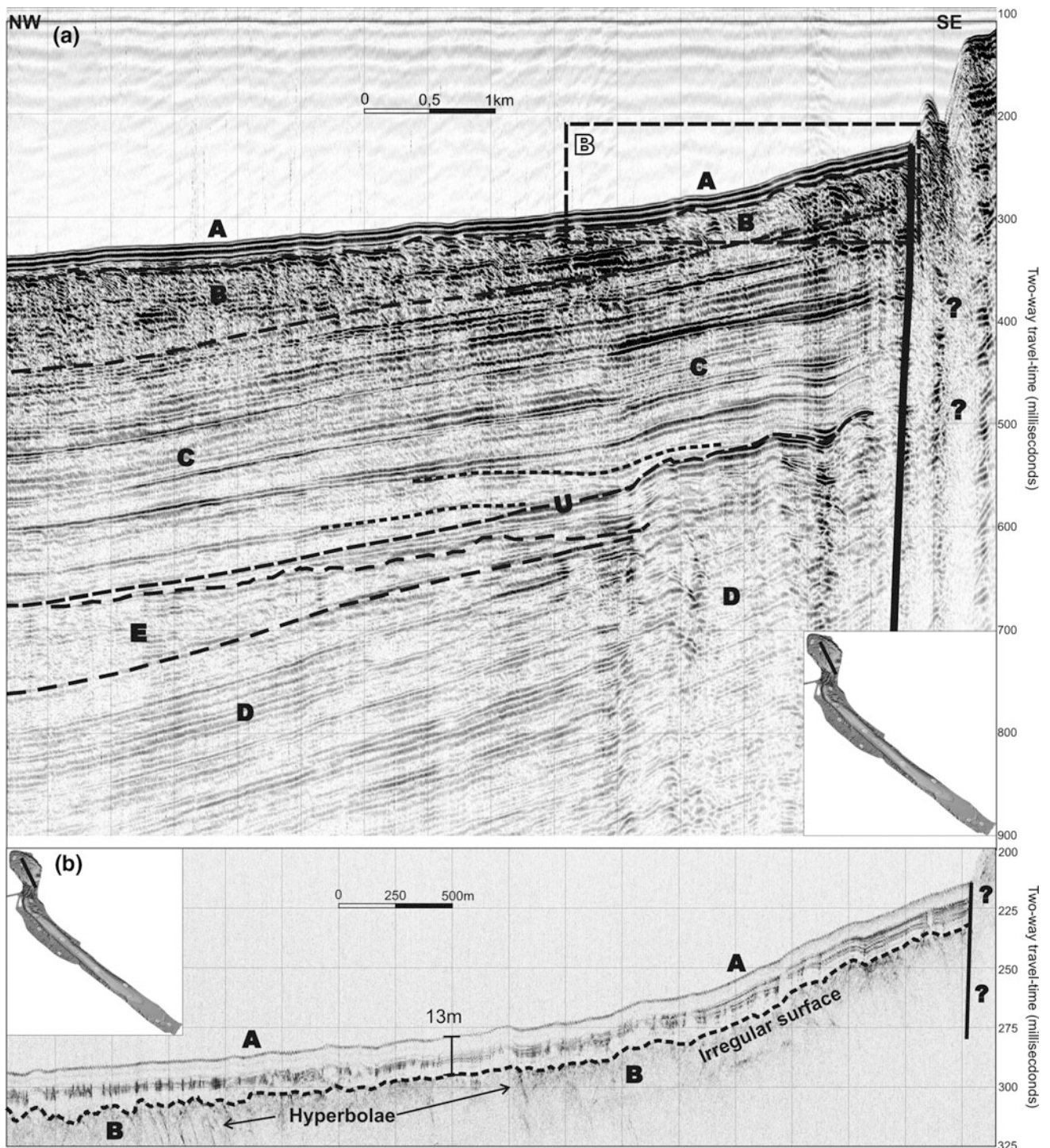


Fig. 13 **a** Airgun 10ci seismic reflection profile from the deep depression in the inner shelf of Farasan Islands. Vertical exaggeration $\times 10$. **b** High resolution subbottom profile from the same depression. Vertical exaggeration $\times 20$. Both profiles have been shot along the same track (see location on Fig. 10). The dashed box in A marks the position of the subbottom profile shown on B

unconformity U. Both packages are characterized by continuous, parallel reflectors, indicating uninterrupted sediment deposition. The seismostratigraphic package E, with

its chaotic to transparent character, may represent a mass failure deposit derived from a possible landslide on the slopes of the depression.

The seismic reflectors of all packages in the seismic profile (Fig. 13a) terminate abruptly against the acoustic basement of the inner shelf. The interface between the sedimentary infill of the depression and the acoustic basement is steep and displays no evidence of active vertical tectonic movement. The age of the sediments deposited in the depression is not known. From their thickness, which exceeds 500 m, it can be assumed that the formation of the depression and the onset of sedimentary deposition may well be of Middle to Lower Pleistocene or even Pliocene age. In

the absence of any age constraints, it is not possible to assess the chronological relationship between the sediments in the depression and the sedimentary formations of the shelf's substrate. The overall shape and structure of the depression strongly suggest that it may represent a sinkhole created due to the solution of a former salt diapir or dome. In addition to the deep depression studied here, a careful examination of the available bathymetric charts (Fig. 2) reveals the existence of several depressions-sinkholes distributed on the Farasan Islands shelf, with similar size, shape and depth.

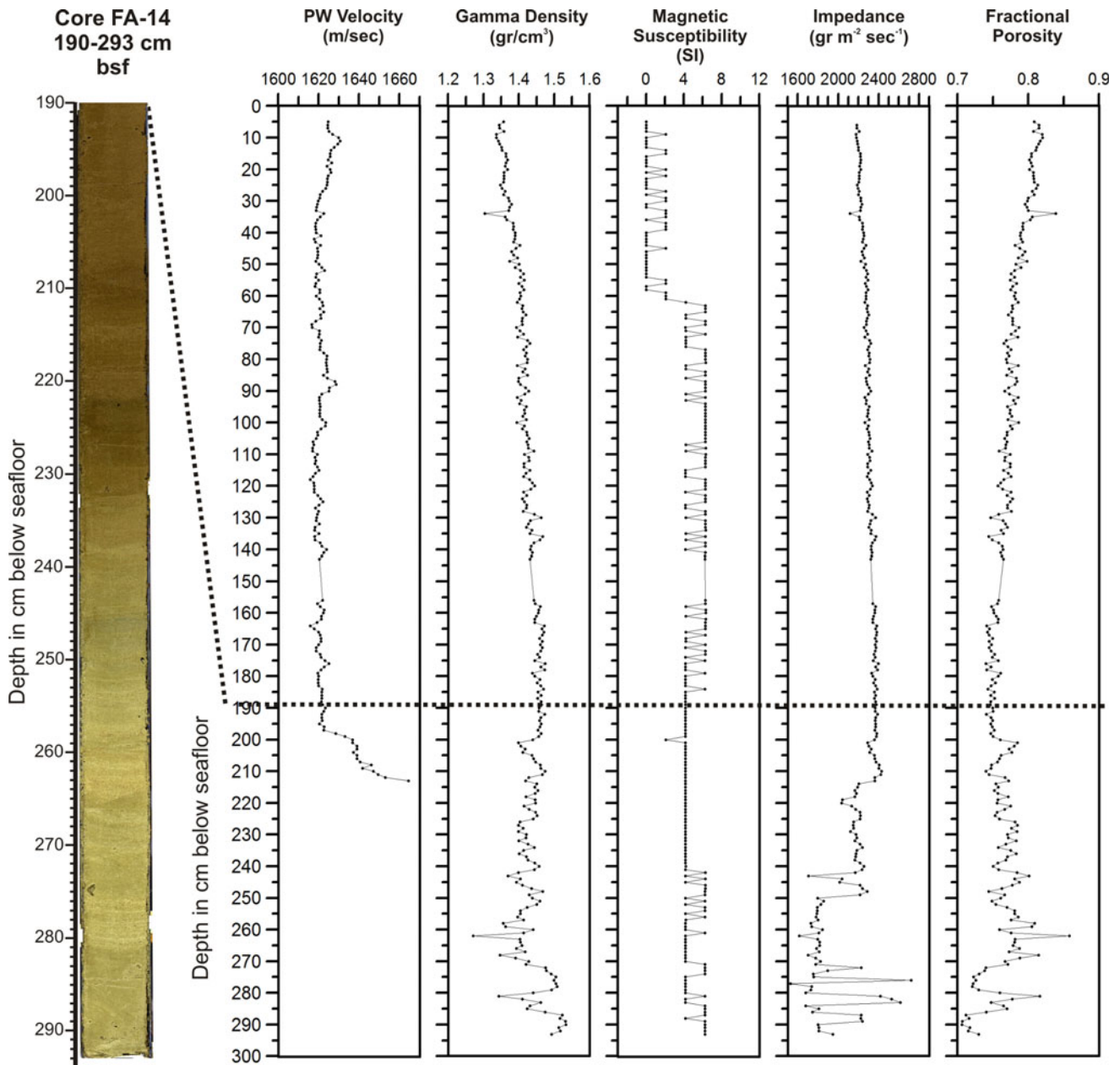


Fig. 14 Physical properties of core FA-14 and photograph of the lower part of the core, between 190 and 293 cm below the seafloor. The location of the core (lat: 17°18.281', long: 41°53.043', depth 245 m) is shown on the map of Fig. 10a. Note the gradual change in sediment colour from olive grey to light greenish grey below 220 cm bsf, which coincides with the change in the other properties at the same depth

Core FA-14 (Fig. 14) confirms a change in the sedimentary environment within the sinkhole, similar to the change observed in the valley of the inner shelf (Fig. 12) as well as in the valley of the outer shelf (Fig. 8). The upper part of the core, between 0 and 230 cm bsf is composed of homogeneous, olive grey silt. Silty sediments persist to the lower end of the core at 293 cm bsf but their colour changes gradually to light greenish grey and remains like that. The physical properties of the sediment, with the exception of the magnetic susceptibility, change down-core too. The gamma density and the fractional porosity show opposite patterns with many variations below 200 cm. The impedance also displays strong variability below 200 cm.

The sedimentological description of the core FA-14 along with the down-core physical properties indicate a gradual change in the depositional environment below 220–230 cm bsf. As with cores FA-12 (Fig. 12) from the valley and FA-5 from the outer shelf (Fig. 8), the upper part of core FA-14

represents homogeneous marine sedimentation during the present high-stand period. The lower part may have been deposited in a different, very probably lacustrine environment, like the one prevailing in the nearby valley.

6.3 Inner Shelf Submerged Landscapes and Palaeoshorelines

The analyses and interpretations of the swath bathymetry, the seismic and subbottom profiling and the sediment coring data presented above lead to interesting results on the palaeo-geomorphological evolution of the inner shelf survey area with respect to Upper Quaternary sea-level fluctuations (Fig. 15).

The seafloor of the Farasan 2 inner shelf survey area lies at about 70–75 m depth and is in general flat, with numerous mounds developed on it. This depth is close to the depth of

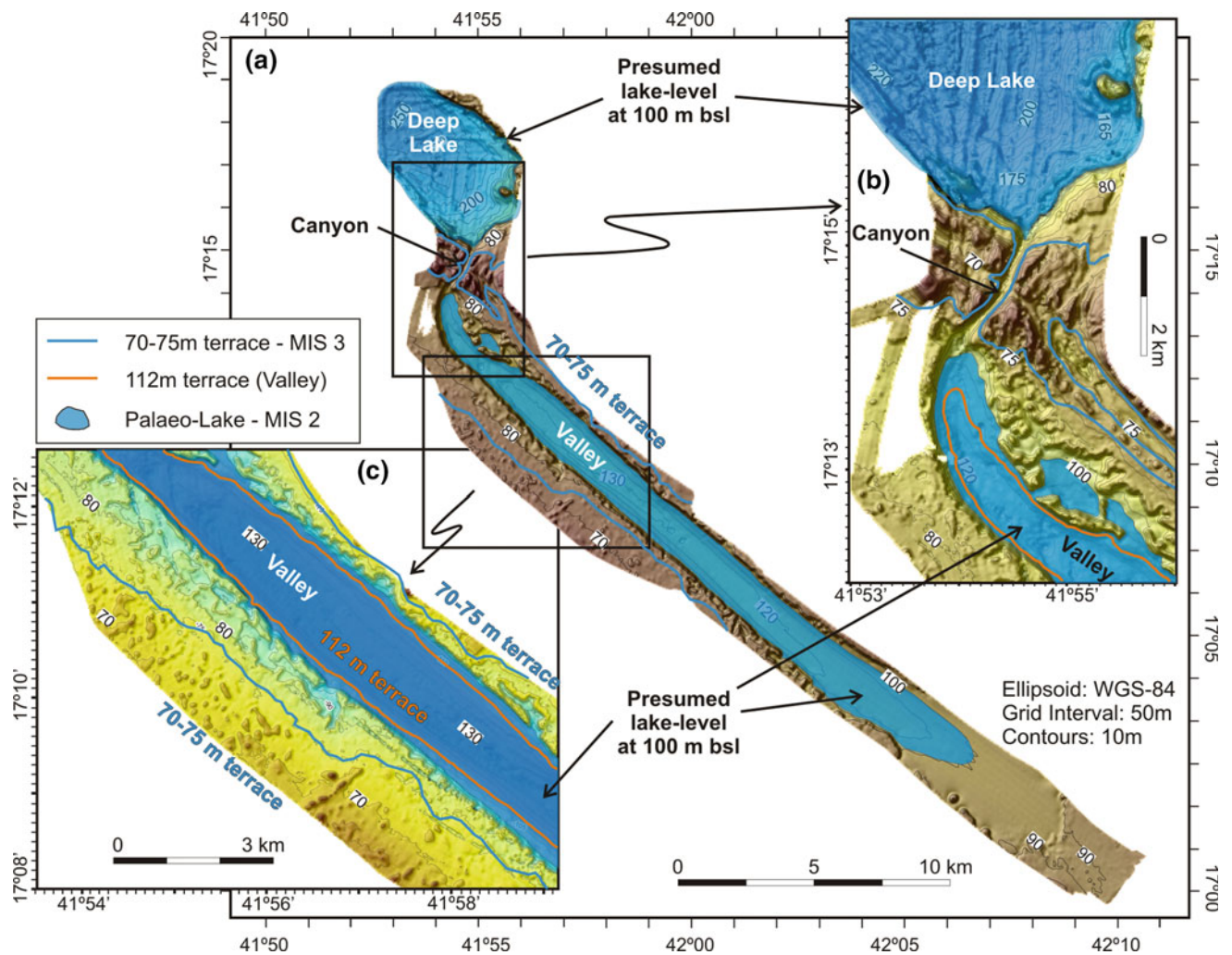


Fig. 15 a Interpretative shaded bathymetry maps of the inner shelf of the Farasan Islands area. b Detailed map and interpretation of the northern part of the survey area. c Detailed map and interpretation of part of the valley

the main terrace mapped on the outer shelf between 70 m and 90 m (Fig. 9) which has been assigned to MIS 3. This is good evidence to suggest that the MIS 3 marine terrace is the one that forms the largest part of the present continental shelf around the Farasan Islands.

Both the long, straight valley and the deep circular to ellipsoidal sinkhole display evidence for a major environmental change at the transition from the LGM to the Holocene high sea-level stand. A morphological terrace at 112 m depth on both sides of the valley, covered by a drape of transparent, recent deposits (Fig. 11), indicates that the valley was filled with water up to this depth in a certain period, possibly during parts of the last low sea-level period. The deposition of lacustrine sediments in the valley has been confirmed with cores FA-12 (Fig. 12) and FA-13. Still, the lacustrine sediments in these cores occur at 106 m and

103 m bsl respectively, which is higher than the observed terrace. This may mean that the lake-level within the valley may have fluctuated by several metres before the area was drowned by the rising sea level. A second possible lake level may be at about 100 m depth, which is the depth of the foot of the steep parts of the slopes of the valley (Fig. 15).

The deep depression to the north of the valley is interpreted as a sinkhole, based on the steepness of the surrounding walls and its shape. It also hosted a lake, as indicated by the bathymetry of the surrounding seafloor and confirmed by the analyses of the sediment in core FA-14 (Fig. 14). Unlike the valley, there is no data to estimate or infer the position of the water-level in the sinkhole. By analogy with the assumed lake-level in the valley, the shoreline of the lake in the sinkhole has been drawn at about 100 m depth on Fig. 15.

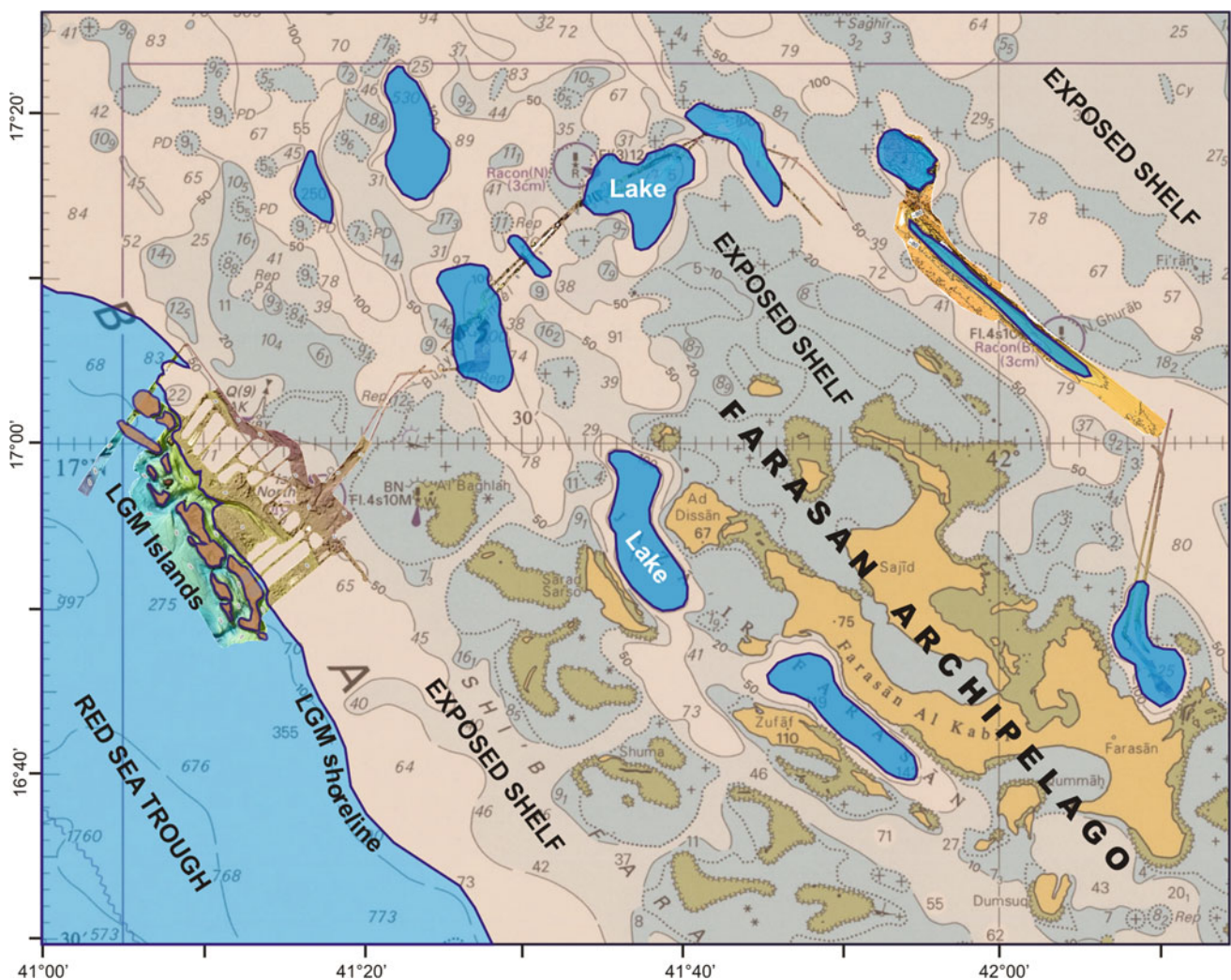


Fig. 16 Palaeogeographic reconstruction of the Farasan Islands shelf during the Last Glacial Maximum. Note the inferred lakes where deep sinkholes occur on the shelf. The LGM shoreline has been drawn at 115–120 m depth. Note the islands (brown colour) at short distance from the LGM shoreline

No matter what was the exact water-level in the valley and the sinkhole, the fact is that during the LGM, when the shelf was subaerially exposed, two lakes, a long and shallow one and a deep and ellipsoidal one, existed on this part of the inner shelf. The analyses of the sediment cores retrieved from both are in progress and so far we have no evidence to indicate whether they were filled with freshwater or not. The narrow, 80 m deep canyon, which connects the northernmost tip of the valley with the southernmost tip of the sinkhole, is fairly clear evidence for erosion due to surface flowing water when the shelf was exposed.

7 Synthesis—Discussion

The observations and results on the geological and tectonic structure, the seismic stratigraphy, the sedimentation and the geomorphological evolution of the two survey areas in the outer and the inner shelf of the Farasan Islands, as presented above, lead to the following conclusions.

The flat part of the Farasan Islands inner and outer shelf, which has been mapped at depths between 70 m and 90 m, dips very gently toward the southwest and may have developed as an erosive marine terrace during the upper half of MIS 3, between 30 and 45 ka BP. This hypothesis is supported by the sea-level curve of Rohling et al. (2013) for the Red Sea. The deeper terrace that has been mapped on the outer shelf at 115–120 m depth corresponds to the sea-level of MIS 2. Thus, the entire shelf may have been subaerially exposed during the LGM (Fig. 16). A shallower terrace, at about 40 m depth, may be correlated with MIS 5.1, 80–85 ka BP, when the sea-level fluctuated between 35 m and 45 m bpsl.

Extensional tectonics, possibly driven by the inferred, basin-ward flow of Miocene evaporite deposits in deeper stratigraphic levels below the shelf, is responsible for the rupturing of the latter with predominantly NW–SE trending normal faults. Dragging of the overlying, faulted, Plio-Quaternary rocks due to the underlying salt flow led to the drifting away of blocks off the shelf edge and the creation of isolated ridges and shoals surrounded by steep slopes and troughs. The 90 m deep flat tops of the ridges and shoals were also subaerially exposed when the sea-level was at 115–120 m bpsl during the Last Glacial Maximum and were islands located at short distances from the shelf edge and the LGM shoreline.

The troughs separating the islands from the shelf host sedimentary sequences, the thickness of which exceeds 150 m. There are not enough constraints to estimate the mean sedimentation rate in the troughs, but it is reasonable to assume that the troughs existed for at least several hundreds of thousands of years. In that case, and if vertical movements can be considered as negligible in the area, then it seems reasonable to assume that the geomorphological

configuration suggested here for MIS 2, with the exposed shelf and the flat-topped palaeo-islands, may also be valid for the previous low sea-level period at 140 ka BP (MIS 6).

Shallow or deep, circular, irregular or elongate depressions and valleys have been mapped on the main terrace of the Farasan Islands shelf. Seismic stratigraphic and sedimentological data confirm that they were filled permanently or ephemerally with water, thus forming lakes, when the shelf was exposed during MIS 2. Geochemical, micropaleontological and radiometric analyses on the sediments retrieved from below the seafloor of these depressions are in progress, aiming at unravelling the environmental conditions prevailing in the LGM lakes, and in particular at resolving whether the lakes were filled with fresh water.

The hydrographic charts of the Farasan Islands shelf show many deep depressions with depths in excess of 200 m, very similar to the one interpreted as a sinkhole lake studied here, in the inner shelf Farasan 2 survey area. If they were lakes too, the 120 km wide and several-hundred-km-long Farasan shelf may have been a place where numerous lakes existed when it was exposed during the LGM (Fig. 16). In addition, the presence of valleys and canyons indicates that surface water run-off eroded the shelf under subaerial conditions. Finally, the seismic stratigraphy observed below the shelf, with horizontal or gently dipping sedimentary layers, may have favoured the development of groundwater aquifers and the occurrence of springs along the slopes of the valleys when subaerially exposed.

Acknowledgements We thank the Saudi Commission for Tourism and National Heritage (SCTH) for permission to undertake fieldwork, and the President, HRH Prince Sultan bin Salman bin AbdulAziz al Saud, the Vice-President, Professor Ali Al-Ghassan, and the Director General, Jamal al Omar, for their support of our research. We also thank HRH King Salman bin Abul Aziz Al Saud, formerly Crown Prince and Minister of Defense, and the Hydrographic Department of the Saudi Ministry of Defense, for permission to undertake the cruise of R/V AEGAEO. We also thank Lt. Fahad Al Shwish, Observer from the Hydrographic Department of the Saudi Ministry of Defense, for his support and valuable assistance in overcoming unexpected logistical difficulties during the cruise, and Captain Theodoros Kanakaris and the crew of R/V AEGAEO for their untiring efforts to ensure the smooth running of the scientific operation during the offshore survey work. The research is funded by the European Research Council through Advanced Grant 269586 DISPERSE under the ‘Ideas’ Specific Programme of the Seventh Framework Programme. This is DISPERSE contribution no. 43.

References

- Abou Ouf MA, El-Shater A (1992) Sedimentology and mineralogy of Jizan shelf sediments, Red Sea, and Saudi Arabia. *J King Abdulaziz Univ Marine Sci Jeddah* 3:39–54
- Armitage SJ, Jasim SA, Marks AE, Parker AG, Usik VI, Uerpmann H-P (2011) The southern route “Out of Africa”: evidence for an

- early expansion of modern humans into Arabia. *Science* 331:453–456
- Augustin N, Devey CW, van der Zwan FM, Feldens P, Tominaga M, Bantan RA, Kwasnitschka T (2014) The rifting to spreading transition in the Red Sea. *Earth Planet Sci Lett* 395:217–230
- Augustin N, Devey N, van der Zwan F (this volume) A modern view on the Red Sea Rift: tectonics, volcanism and salt blankets
- Bailey GN, Flemming NC (2008) Archaeology of the continental shelf: Marine resources, submerged landscapes and underwater archaeology. *Quat Sci Rev* 27:2153–2165
- Bailey GN, King GCP (2011) Dynamic landscapes and human dispersal patterns: tectonics, coastlines and the reconstruction of human habitats. *Quatern Sci Rev* 30:1533–1553
- Bailey GN, Sakellariou D (2012) SPLASHCOS: Submerged Prehistoric Archaeology and Landscapes of the Continental Shelf. *Antiquity* 86(334). <http://antiquity.ac.uk/projgall/sakellariou334/>
- Bailey GN, King GCP, Flemming NC, Lambeck K, Momber G, Moran LJ, Al-Sharekh AM, Vita-Finzi C (2007) Coastlines, submerged landscapes and human evolution: The Red Sea Basin and the Farasan Islands. *J Island Coastal Archaeology* 2:127–160
- Bailey GN, King GCP, Devès M, Hausmann N, Inglis R, Laurie E, Meredith-Williams M, Momber G, Winder I, Alsharekh A, Sakellariou D (2012) DISPERSE: dynamic landscapes, coastal environments and human dispersals. *Antiquity* 86(334). <http://antiquity.ac.uk/projgall/bailey334/>
- Bailey GN, Reynolds SC, King GCP (2011) Landscapes of human evolution: models and methods of tectonic geomorphology and the reconstruction of hominin landscapes. *J Human Evolution* 60(3):257–280
- Bailey GN, Devès MH, Inglis RH, Meredith-Williams MG, Momber G, Sakellariou D, Sinclair AGM, Rousakis G, Al Ghamdi S, Alsharekh AM (2015) Blue Arabia: Palaeolithic and underwater survey in SW Saudi Arabia and the role of coasts in Pleistocene dispersal. *Quatern Int* 382:42–57. <https://doi.org/10.1016/j.quaint.2015.01.002>
- Bailey G, Meredith-Williams M, Alsharekh A, Hausmann N (this volume) The archaeology of Pleistocene coastal environments and human dispersals in the Red Sea: Insights from the Farasan Islands
- Bantan RA (1999) Geology and sedimentary environments of Farasan Bank (Saudi Arabia) southern Red Sea: A combined remote sensing and field study. Ph.D. Thesis, Department of Geology, Royal Holloway, University of London, January 1999
- Bayer HJ, Hotzl H, Jado AR, Roscher B, Voggenreiter W (1988) Sedimentary and structural evolution of the northwest Arabian Red Sea Margin. *Tectonophysics* 153:136–151
- Bosence DWJ (1998) Stratigraphic and sedimentological models of rift basins. In: Purser BH, Bosence DWJ (eds) *Sedimentation and tectonics in Rift basins: Red Sea-Gulf of Aden*. Chapman & Hall, London, pp 9–25
- Bosworth W, Huchon P, McClay K (2005) The Red Sea and Gulf of Aden Basins. *J African Earth Sci* 43:334–378
- Bosworth W (2015) Geological evolution of the Red Sea: Historical background, review, and synthesis. In: Rasul NMA, Stewart ICF (eds) *The Red Sea*. Springer Earth System Sciences, Springer-Verlag Berlin Heidelberg, pp 45–78. https://doi.org/10.1007/978-3-662-45201-1_1
- Carbone F, Matteucci R, Angelucci A (1998) Present day sedimentation of the carbonate platform of the Dahlak Islands, Eritrea. In: Purser BH, Bosence DWJ (eds) *Sedimentation and tectonics in Rift basins, Red Sea-Gulf of Aden*. Chapman & Hall, London, pp 523–536
- Cochran JR (1983) A model for development of the Red Sea. *Bull Am Assoc Petrol Geologists* 67:41–69
- Dabbagh A, Hoetzel H, Schnier H (1984) Farasan Islands. In: Jado AR, Zöttl (eds) *Quaternary Period in Saudi Arabia*. Springer, Wien, pp 212–220
- Delagnes A, Tribolo C, Bertran P, Brenet M, Rémy C, Laubert J, Khalidi L, Mercier N, Nomade S, Peigne S, Sitzia L, Tourne-Piche J-F, Al-Halibi M, Al-Mosabi A, Macchiarelli R (2012) Inland human settlement in southern Arabia 55,000 years ago. New evidence from the Wadi Surdud Middle Paleolithic site complex, western Yemen. *J Human Evolution* 63(3):452–474
- Dixon JE, Monteleone K (2014) Gateway to the Americas: Underwater archaeological survey in Beringia and the North Pacific. In: Evans A, Flemming N, Flatman J (eds) *Prehistoric Archaeology of the Continental Shelf: A Global Review*. Springer, New York, pp 95–114
- Dullo WC (1990) Facies, fossil record and age of Pleistocene reefs from the Red Sea (Saudi Arabia). *Facies* 22:1–46
- Dullo WC, Blomeier D, Camoin GF, Casanova J, Colonna M et al (1997) Morphological evolution and sedimentary facies on the fore-slopes of Mayotte, Comoro Island: Direct observations from submarine. In: Camsin G, Bergerson D (eds) *Carbonate Platforms of the Indian Ocean and the Pacific*. IAS Special Publication
- Dullo WC, Montaggioni L (1998) Modern Red Sea coral reefs: A review of their morphologies and zonation. In: Purser BH, Bosence DWJ (eds) *Sedimentation and Tectonics in Rift Basins: Red Sea-Gulf of Aden*. Chapman & Hall, London, pp 583–594
- Faure H, Walter RC, Grant DR (2002) The coastal oasis: Ice age springs on emerged continental shelves. *Global Planetary Change* 33:47–56
- Feldens P, Mitchell NC (2015) Salt flows in the central Red Sea. In: Rasul NMA, Stewart ICF (eds) *The Red Sea: the formation, morphology, oceanography and environment of a young ocean basin*. Springer Earth System Sciences, Berlin Heidelberg, pp 205–218. https://doi.org/10.1007/978-3-662-45201-1_1
- Geraga M, Sergiou S, Sakellariou D (this volume) Preliminary results of micropaleontological analyses on sediment core FA09 from the southern Red Sea continental shelf
- Girdler RW, Styles P (1974) Two stage sea-floor spreading. *Nature* 247:7–11
- Gvirtzman G (1994) Fluctuations of sea level during the past 400,000 years: the record of Sinai, Egypt (Northern Red Sea). *Coral Reefs* 13:203–214
- Hudec MR, Jackson MPA (2007) Terra infirma: Understanding salt tectonics. *Earth-Sci Rev* 82:1–28
- Hughes GW, Beydoun ZR (1992) The Red Sea-Gulf of Aden: Biostratigraphy, lithostratigraphy and palaeoenvironments. *J Petrol Geol* 15:135–156
- Inglis RH, Bosworth W, Rasul N, Al Saedi A, Bailey G (this volume) Investigating the palaeoshorelines and coastal archaeology of the southern Red Sea
- King GCP, Bailey GN (2006) Tectonics and human evolution. *Antiquity* 80:265–286
- LaBreque JL, Zitellini N (1985) Continuous sea-floor spreading in Red Sea, an alternative interpretation of magnetic anomaly pattern. *Bull Am Assoc Petrol Geol* 69:513–524
- Lambeck K, Purcell A, Flemming N, Vita-Finzi C, Alsharekh A, Bailey GN (2011) Sea level and shoreline reconstructions for the Red Sea: Isostatic and tectonic considerations and implications for hominin migration out of Africa. *Quatern Sci Rev* 30:3542–3574
- Macaulay V, Hill C, Achilli A, Rengo C, Clarke D, Meehan W, Blackburn J, Semino O, Scozzari R, Cruciani F, Taha A, Shaari NK, Raja JM, Ismail P, Zainuddin Z, Goodwin W, Bulbeck D, Bandelt HJ, Oppenheimer S, Torroni A, Richards M (2005) Single, rapid coastal settlement of Asia revealed by analysis of complete mitochondrial genomes. *Science* 308:1034–1036

- Mellars P (2006) Why did modern populations disperse from Africa ca. 60,000 years ago? A new model. *Proc Nat Acad Sci USA* 103:9381–9386
- Mideast Industries Ltd. (1966) Salt production possibilities of the Jizan and Farasan Island area. Saudi Arabian Directorate General for Mineral Resource Report DGMR-279, 13 pp
- Mitchell DJW, Allen RB, Salama W, Abduzakm A (1992) Tectonostratigraphic framework and hydrocarbon potential of the Red Sea. *J Petrol Geol* 15(2):187–210
- Petraglia MD, Rose JI (eds) (2009) *The evolution of human populations in Arabia*. Springer, Dordrecht
- Petraglia MD, Alsharekh AM, Crassard E, Drake NA, Groucutt H, Parker AG, Roberts RG (2011) Middle Paleolithic occupation on a Marine Isotope Stage 5 lakeshore in the Nefud Desert. Saudi Arabia. *Quatern Sci Rev* 30(13–14):1555–1559
- Petraglia MD, Breeze PS, Groucutt HS (this volume) *Blue Arabia, Green Arabia: Examining human colonisation and dispersal models*
- Purser BH, Bosence DWJ (1999) *Sedimentation and tectonics in rift basins: Red Sea-Gulf of Aden*. Chapman & Hall, London
- Roeser HA (1975) A detailed magnetic survey of the southern Red Sea. *Geol. Jb.* D13:131–153
- Rohling EJ, Fenton M, Jorissen FJ, Bertrand P, Ganssen G, Caulet JP (1998) Magnitudes of sea-level lowstands of the past 500,000 years. *Nature* 394:162–165
- Rohling EJ, Grant K, Bolshaw M, Roberts AP, Siddall M, Hemleben C, Kucera M (2009) Antarctic temperature and global sea level closely coupled over the past five glacial cycles. *Nat Geosci* 2:500–504
- Rohling EJ, Grant KM, Roberts AP, Larrasoana JC (2013) Paleoclimate variability in the Mediterranean and Red Sea regions during the last 500,000 years: Implications for hominin migrations. *Curr Anthropol* 54(S8):S183–S201. <https://doi.org/10.1086/673882>
- Rose JI, Usik V, Marks A, Hilbert Y, Galletti C, Parton A, Geiling JM, V. Cerné V, Morley M, Roberts R (2011) The Nubian complex of Dhofar, Oman: an African Middle Stone Age industry in southern Arabia. *PLoS ONE* 6(11):e28239. <https://doi.org/10.1371/journal.pone.0028239>
- Sanderson D, Kinnaird T (this volume) *Optically Stimulated Luminescence dating as a geochronological tool for Late Quaternary sediments in the Red Sea region*
- Schmidt DL, Hadley DG, Brown GF (1982) Middle Tertiary continental rift and evolution of the Red Sea in south-western Saudi Arabia. Ministry of Petroleum and Mineral Resources, Deputy Ministry for Mineral Resources, Jeddah, USGS-OF-03-6, 56 pp
- Searle RC, Ross DA (1975) A geophysical study of the Red Sea axial trough between 20.5 and 22 N. *Geophys J Roy Astron Soc* 43:555–572
- Siddall M, Smeed DA, Hemleben C, Rohling EJ, Schmelzer I, Peltier WR (2004) Understanding the Red Sea response to sea level. *Earth Planet Sci Lett* 225:421–434
- Stoffers P, Kuhn R (1974) Red Sea evaporites - A petrographic and geochemical study. In: Whitmarsh RB, Weser OE, Ross DA (eds) *Initial reports of the Deep Sea Drilling Project*, vol. 23. U. S. Government. Printing Office, Washington, pp 821–847
- Stoffers P, Ross DA (1977) Sedimentary history of the Red Sea. In: Hilpert LS (ed) *Red Sea Research 1970–1975*. Saudi Arabian Ministry of Petroleum and Mineral Resources, Directorate General of Mineral Resources, Jeddah, Bulletin 22, pp i–iv and H1–H19
- Walter RC, Buffler RT, Bruggemann JJ, Guillaume MMM, Berhe SM, Negassi B, Libsekal Y, Cheng H, Edwards RL, Von Gosele R, Neradeau D, Gagnon M (2000) Early human occupation of the Red Sea coast of Eritrea during the Last Interglacial. *Nature* 405:65–69